

Efficient Temporal Pattern Mining in Big Time Series Using Mutual Information

Van Long Ho*, Nguyen Ho*, Torben Bach Pedersen*
Department of Computer Science, Aalborg University, Denmark
*{vlh, ntth, tbp}@cs.aau.dk

Abstract—Very large time series are increasingly available from an ever wider range of IoT-enabled sensors deployed in different environments. Significant insights can be obtained through mining temporal patterns from these time series. Unlike traditional pattern mining, temporal pattern mining (TPM) adds additional temporal aspect into extracted patterns, thus making them more expressive. However, adding the temporal dimension into patterns results in an exponential growth of the search space, significantly increasing the mining process complexity. Current TPM approaches either cannot scale to large datasets, or typically work on pre-processed event sequences rather than directly on time series. This paper presents our comprehensive Frequent Temporal Pattern Mining from Time Series (FTPMfTS) approach which provides the following contributions: (1) The end-to-end FTPMfTS process that directly takes time series as input and produces frequent temporal patterns as output. (2) The efficient Hierarchical Temporal Pattern Graph Mining (HTPGM) algorithm that uses efficient data structures to enable fast computations for support and confidence. (3) A number of pruning techniques for HTPGM that yield significantly faster mining. (4) An approximate version of HTPGM which relies on mutual information to prune unpromising time series, and thus significantly reduce the search space. (5) An extensive experimental evaluation on real-world datasets from the energy and smart city domains which shows that HTPGM outperforms the baselines, consumes less memory and can scale to big datasets. The approximate HTPGM achieves up to 3 orders of magnitude speedup compared to the baselines while obtaining high accuracy compared to the exact HTPGM.

I. INTRODUCTION

Rapid advancements in IoT technology have enabled the collection of enormous amounts of time series at unprecedented scale and speed. For example, modern residential households are now equipped with smart meters and smart plugs, enabling fine-grained monitoring of the energy consumption of electrical appliances, or weather stations can have thousands of sensors to monitor hundreds of different variables related to weather conditions, generating terabytes of data every day. Analyzing these massive, heterogeneous and rich time series can help uncover hidden patterns and extract new insights to support decision making and optimization.

As an example, consider Fig. 1 that shows the energy consumption time series of electrical appliances in a residential household. Such time series can be analyzed to identify how residents are interacting with electrical appliances in order to understand their living habits. From Fig. 1, a pattern of activations between Kitchen, Toaster and Microwave can be identified which shows that these devices are often used together, usually in the early morning and evening. Such

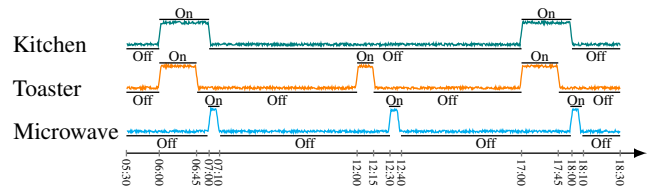


Fig. 1: Energy consumption time series of electrical appliances insights are important, as they can be used to enable the building of smart houses, and/or optimize residential energy usage. For instance, knowing that a resident always showers at 6:00 would enable pre-heating of hot water, e.g., when surplus wind energy is available.

Extracting such patterns is the task of pattern mining, an important branch in data mining. However, traditional pattern mining methods do not fully capture the temporal dimension. For example, sequential pattern mining would express the relation between appliances in Fig. 1 as $\{Kitchen\ On\} \Rightarrow \{Toaster\ On, Microwave\ On\}$, indicating that the occurrence of $\{Toaster\ On, Microwave\ On\}$ is associated with the occurrence of $\{Kitchen\ On\}$. Such expressions omit the pattern occurrence times, and thus, leave out important information.

To overcome this limitation, a recent trend in pattern mining is to add temporal aspects into extracted patterns, forming a group of methods called *temporal pattern mining* (TPM). Using TPM, the previous pattern can be expressed as: $[06:00,07:00] Kitchen\ On \Rightarrow [06:01,06:45] Toaster\ On \Rightarrow [07:00,07:10] Microwave\ On$, or $[1\ hour] Kitchen\ On \Rightarrow_{\text{after } 1\ min} [44\ minutes] Toaster\ On \Rightarrow_{\text{after } 15\ min} [10\ minutes] Microwave\ On$. This type of patterns provides further details on when the relations between events happen, and for how long, making temporal patterns more expressive.

Although temporal patterns are useful, mining them is much more expensive than sequential patterns. Not only does the temporal information add extra computation to the mining process, the complex relations between events also result in an exponential growth of the search space, thus significantly increasing the mining complexity. Current existing works such as [1–3], have tried to either use different representations such as augmented hierarchical representation to reduce the relation complexity, or propose different optimizations to improve TPM performance. However, these methods do not scale on big datasets as the challenge of the exponential search space still exists, and/or do not work directly on time series but rather on pre-processed event sequences.

Contributions. In the present paper, we present a compre-

hensive Frequent Temporal Pattern Mining from Time Series (FTPMfTS) approach to overcome the above limitations. Our solution provides the following key contributions. (1) We present the first end-to-end FTPMfTS process that receives a set of time series as input, and produces frequent temporal patterns as output. Within this process, a splitting strategy is proposed to convert time series into event sequences while ensuring the preservation of temporal patterns. (2) We provide a formal definition of temporal patterns through event instances, thus provide a more precise representation of the relations between events. Moreover, we simplify Allen’s relation model for better usefulness and extend it with a buffer-based solution to solve the exact time mapping problem, while ensuring that temporal relations are mutually exclusive. (3) We propose an efficient Hierarchical Temporal Pattern Graph Mining (HTPGM) method to efficiently mine frequent temporal patterns. HTPGM has several important novelties. First, HTPGM employs efficient data structures, Hierarchical Pattern Graph and *bitmap*, to enable fast computations for support and confidence of temporal patterns. Second, two groups of pruning techniques based on the Apriori principle and the transitivity property of temporal relations are proposed to enable faster mining. (4) Based on mutual information, we propose an approximate version of HTPGM that can prune unpromising time series, and thus significantly reduce the search space. This approximation allows HTPGM to scale on big datasets (e.g., many attributes). (5) We perform an extensive experimental evaluation on real-world datasets which shows that HTPGM outperforms the baselines, consumes less memory and can scale to big datasets. The approximate HTPGM achieves up to 3 orders of magnitude speedup while obtaining high accuracy compared to the exact HTPGM.

Paper outline. Section II covers related work. Section III presents relevant concepts and defines the problem. Sections IV and V present the exact and approximate mining methods. Section VI shows experimental evaluation and Section VII concludes the paper.

II. RELATED WORK

Temporal pattern mining: Compared to sequential pattern mining, there is less work that investigates the TPM problem. One of the first work in this area is the proposal of Kam et al. [4] that uses a hierarchical representation to manage temporal relations, and based on that to mine temporal patterns. This approach however suffers from ambiguity when presenting temporal relations. To overcome this, Wu et al. [5] define new non-ambiguous temporal relations, and develop a method called TPprefix to mine temporal patterns. TPprefix however has several inherent limitations: it scans the database repeatedly, and the algorithm does not employ any pruning strategies to reduce the search space. In [6], Moskovitch et al. design a TPM algorithm using the transitivity property of temporal relations. They use this property to generate candidates by inferring new relations between events. This differs from HTPGM as we also use the transitivity property but for pruning. In [7], Iyad et al. propose a temporal pattern mining

framework to detect events in time series. Their focus however is to find irregularities in the data. Iyad et al. [8] propose a TPM algorithm to classify health record data. Campbell et al. [9] introduce a temporal condition pattern mining method to characterize pediatric asthma. However, these approaches are very domain-specific, thus cannot generalize to other domains.

State of the art methods that currently achieve the best performance in TPM are H-DFS [3], TPMiner [1], and IEMiner [2]. H-DFS [3], proposed by Papapetrou et al., is a hybrid algorithm that uses both bread-first and depth-first search strategies to mine frequent arrangements of temporal intervals. H-DFS uses a data structure called ID-List to transform event sequences into vertical representations of events. The ID-Lists of different events are merged in order to generate temporal patterns. This makes H-DFS does not scale well when the data size increases. In [2], Patel et al. design a hierarchical lossless representation to model relations between events, and propose an efficient algorithm called IEMiner that uses Apriori-based optimizations to efficiently mine patterns from this lossless representation. In [1], Chen et al. propose endpoint and end-time representations to simplify the complex relations among events, and design the TPMiner algorithm to mine temporal patterns. Similar to [3], IEMiner and TPMiner do not scale with the increasing of data sizes. Our HTPGM algorithm improves on these methods in the following aspects: (1) we simplify the types of temporal relations in order to reduce the relation complexity, while still ensuring the exclusiveness and completeness of event relations, (2) we use efficient data structures to support fast mining, (3) we propose a number of pruning techniques based on the Apriori principle and the transitivity property of temporal relations to reduce the search space, and (4) we propose an approximate HTPGM in order to handle big datasets.

Using correlations in temporal pattern mining: There have been a few attempts to apply different correlation measures such as expected support [10], all-confidence [11], and mutual information [12–15] to optimize the pattern mining process. However, these only support sequential pattern mining. To the best of our knowledge, our proposed approximate HTPGM is the first to use mutual information for temporal pattern mining.

III. PRELIMINARIES

A. Temporal Event of Time Series

Definition 3.1 (Time series) A *time series* $X = x_1, x_2, \dots, x_n$ is a sequence of data values that measure the same phenomenon during an observation time period, and are chronologically ordered.

Definition 3.2 (Symbolic representation of a time series) A *symbolic representation* \mathcal{X}_S of a time series X encodes the raw values of X to a sequence of symbols. A finite set of permitted symbols used to encode X is called the *symbol alphabet* of X , denoted as Σ_X .

The symbolic representation \mathcal{X}_S can be easily obtained by using a mapping function $f : X \rightarrow \Sigma_X$ that maps each value $x_i \in X$ to a symbol $\omega \in \Sigma_X$.

As an example, assume $X = 1.61, 1.21, 0.41, 0.0$ is a time series representing the energy consumption of an electrical

device. Using the symbol alphabet $\Sigma_X = \{\text{On}, \text{Off}\}$, where On represents the device is on and operating (e.g., when $x_i \geq 0.5$), and Off when the device is off ($x_i < 0.5$), we can obtain the symbolic representation of X as: $\mathcal{X}_S = \text{On}, \text{On}, \text{Off}, \text{Off}$.

Definition 3.3 (Symbolic database) Given a set of time series $\mathcal{X} = \{X_1, \dots, X_n\}$, the collection of symbolic representations of the time series in \mathcal{X} forms a *symbolic database* \mathcal{D}_{SYB} .

Table I is an example of a symbolic database \mathcal{D}_{SYB} containing a set of 6 time series representing the energy consumption of 6 electrical appliances: {Kitchen, Toaster, Microwave, Coffee Machine, Clothes Ironer, and Blender}. For brevity, we name the appliances as {K, T, M, C, I, B}, respectively. All appliances have the same alphabet $\Sigma = \{\text{On}, \text{Off}\}$.

Definition 3.4 (Temporal event in a time series) A *temporal event* E in a time series X is a tuple $E = (\omega, T)$ where $\omega \in \Sigma_X$ is a symbol, and $T = \{[t_{s_i}, t_{e_i}]\}$ is a set of time intervals during which X is associated with the symbol ω .

Given a symbolic representation \mathcal{X}_S , a temporal event in X is formed by combining identical consecutive symbols in \mathcal{X}_S into one time interval. For example, consider the symbolic representation of K in Table I. We can combine its consecutive On symbols to form the temporal event “Kitchen is On” as: (KOn, $\{[10:00, 10:15], [10:35, 10:40], [11:15, 11:25], [11:50, 12:00], [12:15, 12:20], [12:35, 12:45]\}$).

Definition 3.5 (Instance of a temporal event) Let $E = (\omega, T)$ be a temporal event, and $[t_{s_i}, t_{e_i}] \in T$ be a time interval. The tuple $e = (\omega, [t_{s_i}, t_{e_i}])$ is called an *instance* of the event E , representing a single occurrence of E during $[t_{s_i}, t_{e_i}]$. We use $E_{\triangleright e}$ to denote that event E has an instance e .

B. Relations between Temporal Events

To find temporal patterns, we need to define the relations between temporal events, which we adopt a popular relation model proposed by Allen [16]. However, we simplify Allen’s relations, reducing the 7 original relations into 3 basic ones, while still maintaining a similar expressive power. Moreover, to avoid the exact time mapping problem in Allen model, we adopt the buffer idea in [3] that adds a *buffer* ϵ to the relation’s endpoints as a tolerant duration. However, we change the way ϵ is used to ensure that relations are mutually exclusive.

Consider two temporal events E_1 and E_2 , and their corresponding instances, e_1 occurring during $[t_{s_1}, t_{e_1}]$ and e_2 occurring during $[t_{s_2}, t_{e_2}]$. Let ϵ be a non-negative number ($\epsilon \geq 0$) representing the buffer value. The following relations can be defined between E_1 and E_2 through e_1 and e_2 .

Definition 3.6 (Follow) Two temporal events E_1 and E_2 form a *Follow* relation through e_1 and e_2 , denoted as Follows($E_{1 \triangleright e_1}, E_{2 \triangleright e_2}$) or $E_{1 \triangleright e_1} \rightarrow E_{2 \triangleright e_2}$, iff $t_{e_1} \pm \epsilon \leq t_{s_2}$.

Definition 3.7 (Contain) Two temporal events E_1 and E_2 form a *Contain* relation through e_1 and e_2 , denoted as Contains($E_{1 \triangleright e_1}, E_{2 \triangleright e_2}$) or $E_{1 \triangleright e_1} \supseteq E_{2 \triangleright e_2}$, iff $(t_{s_1} \leq t_{s_2}) \wedge (t_{e_1} \pm \epsilon \geq t_{e_2})$.

Definition 3.8 (Overlap) Two temporal events E_1 and E_2 form an *Overlap* relation through e_1 and e_2 , denoted as Overlaps($E_{1 \triangleright e_1}, E_{2 \triangleright e_2}$) or $E_{1 \triangleright e_1} \overline{\cap} E_{2 \triangleright e_2}$, iff $(t_{s_1} < t_{s_2}) \wedge (t_{e_1} \pm \epsilon < t_{e_2}) \wedge (t_{e_1} - t_{s_2} \geq d_o \pm \epsilon)$, where d_o is a

positive number representing the minimal overlapping duration between two event instances: $0 \leq \epsilon \ll d_o$.

Table II illustrates the three temporal relations. Since the relations between events are formed through their instances, it is possible that the same event pair forms different relations through different instances, or an event can form the relation with itself. In this case, we call it a *self-relation*.

C. Temporal Pattern

Definition 3.9 (Temporal sequence) A list of event instances $S = \langle e_1, \dots, e_i, \dots, e_n \rangle$ forms a *temporal sequence* if the event instances are chronologically ordered by their start times. Moreover, S has size n , denoted as $|S| = n$.

Definition 3.10 (Temporal sequence database) A collection of temporal sequences forms a *temporal sequence database* \mathcal{D}_{SEQ} where each row i contains a temporal sequence S_i .

Table III is an example of temporal sequence database \mathcal{D}_{SEQ} , created from the symbolic database \mathcal{D}_{SYB} in Table I.

Definition 3.11 (Temporal pattern) Let $\mathfrak{R} = \{\text{Follow}, \text{Contain}, \text{Overlap}\}$ be the set of relations between temporal events. A *temporal pattern* $P = \langle (E_1, r_{12}, E_2), \dots, (E_{n-1}, r_{(n-1)(n)}, E_n) \rangle$ is a list of triples (E_i, r_{ij}, E_j) , each represents a relation $r_{ij} \in \mathfrak{R}$ between two events E_i and E_j .

A temporal pattern that has n events is called an n -event pattern. For the notation, we use $E_i \in P$ to denote that the event E_i occurs in P , and $P_1 \subseteq P$ to say that the temporal pattern P_1 is a sub-pattern of P .

Definition 3.12 (Temporal sequence supports a pattern) Let $S = \langle e_1, \dots, e_i, \dots, e_n \rangle$ be a temporal sequence. We say that S supports a temporal pattern P , denoted as $P \in S$, iff $|S| \geq 2 \wedge \forall (E_i, r_{ij}, E_j) \in P, \exists (e_l, e_m) \in S$ such that r_{ij} holds between $E_{i \triangleright e_l}$ and $E_{j \triangleright e_m}$. If P is supported by S , P can be written in the form $P = \langle (E_{1 \triangleright e_1}, r_{12}, E_{2 \triangleright e_2}), \dots, (E_{n-1 \triangleright e_{n-1}}, r_{(n-1)(n)}, E_{n \triangleright e_n}) \rangle$, where the relation between events in each triple is expressed using the event instances.

In Fig. 1, the temporal sequence $S = \langle (\text{KOn}, [06:00, 07:00]), (\text{TOOn}, [06:01, 06:45]), (\text{MOn}, [07:00, 07:10]) \rangle$ represents a chronological order of appliances’ activations in a household, and S supports a 3-event pattern $P = \langle (\text{KOn}, \text{Contain}, \text{TOOn}), (\text{KOn}, \text{Follow}, \text{MOn}), (\text{TOOn}, \text{Follow}, \text{MOn}) \rangle$.

Constraint on maximal duration of a pattern: Let $P \in S$ be a temporal pattern supported by the sequence S . The duration between the start time of the instance e_1 , and the end time of the instance e_n in S must not exceed the predefined maximal time duration t_{max} : $t_{e_n} - t_{s_1} \leq t_{\text{max}}$.

The maximal duration constraint guarantees that the relation between any two events is temporally valid. This enables the pruning of invalid patterns. For example, under this constraint, a *Follow* relation between a “Kitchen On” event and a “Toaster On” event happened one year apart should be considered invalid.

D. Frequent Temporal Pattern

Given a temporal sequence database \mathcal{D}_{SEQ} , we want to find temporal patterns that occur frequently in \mathcal{D}_{SEQ} . We use *support* and *confidence* to measure the frequency of a pattern.

TABLE I: A Symbolic Database \mathcal{D}_{SYB}

| Time | 10:00 | 10:05 | 10:10 | 10:15 | 10:20 | 10:25 | 10:30 | 10:35 | 10:40 | 10:45 | 10:50 | 10:55 | 11:00 | 11:05 | 11:10 | 11:15 | 11:20 | 11:25 | 11:30 | 11:35 | 11:40 | 11:45 | 11:50 | 11:55 | 12:00 | 12:05 | 12:10 | 12:15 | 12:20 | 12:25 | 12:30 | 12:35 | 12:40 | 12:45 | 12:50 | 12:55 |
|------|-------|-------|-------|-------|-------|-------|-------|-------|-------|-------|-------|-------|-------|-------|-------|-------|-------|-------|-------|-------|-------|-------|-------|-------|-------|-------|-------|-------|-------|-------|-------|-------|-------|-------|-------|-------|
| K | On | On | On | On | Off | Off | Off | On | On | Off | Off | Off | Off | Off | On | On | On | On | Off | Off | Off | Off | On | On | On | Off | Off | On | On | Off | Off | On | On | On | Off | Off |
| T | Off | On | On | On | Off | Off | Off | On | On | Off | Off | On | On | Off | Off | On | On | On | Off | Off | Off | Off | On | On | On | Off | Off | On | On | Off | Off | Off | On | On | On | Off |
| M | Off | Off | Off | Off | On | On | On | Off | Off | On | On | On | Off | On | On | Off | Off | Off | On | On | Off | On | On | Off | Off | On | On | Off | Off | On | On | On | Off | Off | On | On |
| C | Off | Off | Off | Off | On | On | On | Off | Off | On | On | Off | On | On | On | Off | Off | Off | On | On | Off | On | On | Off | Off | On | On | Off | Off | On | On | On | Off | Off | On | On |
| I | Off | On | On | Off | Off | Off | Off | On | On | Off | On | On | Off | Off | Off | On | On | Off | Off | |
| B | Off | On | On | Off | On | On | Off | On | On | Off | Off | Off | Off | Off | Off | On | |

TABLE II: Temporal Relations between Events

| | |
|---|---|
| Follow relation: $E_{1 \triangleright e_1} \rightarrow E_{2 \triangleright e_2}$ | $t_{s_1} \quad e_1 \quad t_{e_1} \pm \epsilon \quad e_2 \quad t_{s_2} \quad t_{e_2}$ $t_{e_1} \pm \epsilon \leq t_{s_2}$ |
| Contain relation: $E_{1 \triangleright e_1} \supset E_{2 \triangleright e_2}$ | $t_{s_1} \quad e_1 \quad t_{e_1} \pm \epsilon \quad t_{s_2} \quad e_2 \quad t_{e_2}$ $t_{s_1} \leq t_{s_2} \wedge (t_{e_1} \pm \epsilon \geq t_{e_2})$ |
| Overlap relation: $E_{1 \triangleright e_1} \cap E_{2 \triangleright e_2}$ | $t_{s_1} \quad e_1 \quad t_{e_1} \pm \epsilon \quad t_{s_2} \quad e_2 \quad t_{e_2}$ $(t_{s_1} < t_{s_2}) \wedge (t_{e_1} \pm \epsilon < t_{e_2}) \wedge (t_{e_1} - t_{s_2} \geq d_0 \pm \epsilon)$ |

 TABLE III: A Temporal Sequence Database \mathcal{D}_{SEQ}

| ID | Temporal sequences |
|----|--|
| 1 | (KOn,[10:00,10:15]), (KOff,[10:15,10:35]), (KOn,[10:35,10:40]), (TOff,[10:00,10:05]), (TON,[10:05,10:15]), (TOff,[10:15,10:35]), (TON,[10:35,10:40]), (MOff,[10:00,10:20]), (MON,[10:20,10:30]), (MOff,[10:30,10:40]), (COff,[10:00,10:20]), (CON,[10:20,10:30]), (COff,[10:30,10:40]), (IOff,[10:00,10:40]), (BOff,[10:00,10:35]), (BOn,[10:35,10:40]) |
| 2 | (KOff,[10:45,11:15]), (KOn,[11:15,11:25]), (TOff,[10:45,10:55]), (TON,[10:55,11:00]), (TOff,[11:00,11:15]), (TON,[11:15,11:25]), (MON,[10:45,10:55]), (MOff,[10:55,11:05]), (MON,[11:05,11:10]), (MOff,[11:10,11:25]), (CON,[10:45,10:50]), (COff,[10:50,11:00]), (CON,[11:00,11:10]), (COff,[11:10,11:25]), (ION,[10:45,10:50]), (IOff,[10:50,11:20]), (ION,[11:20,11:25]), (BOff,[10:45,11:25]) |
| 3 | (KOff,[11:30,11:50]), (KOn,[11:50,12:00]), (KOff,[12:00,12:10]), (TOff,[11:30,11:50]), (TON,[11:50,12:00]), (TOff,[12:00,12:10]), (MON,[11:30,11:35]), (MOff,[11:35,11:45]), (MON,[11:45,11:50]), (MOff,[11:50,12:05]), (MON,[12:05,12:10]), (CON,[11:30,11:35]), (COff,[11:35,11:45]), (CON,[11:45,11:50]), (COff,[11:50,12:05]), (CON,[12:05,12:10]), (IOff,[11:30,12:10]), (BOn,[11:30,11:35]), (BOff,[11:35,12:10]) |
| 4 | (KOn,[12:15,12:20]), (KOff,[12:20,12:35]), (KOn,[12:35,12:45]), (KOff,[12:45,12:55]), (TON,[12:15,12:20]), (TOff,[12:20,12:40]), (TON,[12:40,12:50]), (TOff,[12:50,12:55]), (MOff,[12:15,12:25]), (MON,[12:25,12:35]), (MOff,[12:35,12:50]), (MON,[12:50,12:55]), (COff,[12:15,12:25]), (CON,[12:25,12:35]), (COff,[12:35,12:50]), (CON,[12:50,12:55]), (ION,[12:15,12:20]), (IOff,[12:20,12:40]), (ION,[12:40,12:45]), (IOff,[12:45,12:55]), (BOn,[12:15,12:20]), (BOff,[12:20,12:50]), (BOn,[12:50,12:55]) |

Definition 3.13 (Support of a temporal event) The *support* of a temporal event E in \mathcal{D}_{SEQ} is the number of temporal sequences $S \in \mathcal{D}_{\text{SEQ}}$ that contain at least one instance of E .

$$\text{supp}(E) = |\{S \in \mathcal{D}_{\text{SEQ}} \text{ s.t. } \exists e \in S : E \triangleright e\}| \quad (1)$$

The *relative support* of E is the fraction between $\text{supp}(E)$ and the size of \mathcal{D}_{SEQ} :

$$\text{rel-supp}(E) = \text{supp}(E) / |\mathcal{D}_{\text{SEQ}}| \quad (2)$$

Similarly, the support of a group of events (E_1, \dots, E_n) , denoted as $\text{supp}(E_1, \dots, E_n)$, is the number of sequences $S \in \mathcal{D}_{\text{SEQ}}$ which contain at least one instance of the group.

Definition 3.14 (Support of a temporal pattern) The *support* of a temporal pattern P is the number of temporal sequences $S \in \mathcal{D}_{\text{SEQ}}$ that support P .

$$\text{supp}(P) = |\{S \in \mathcal{D}_{\text{SEQ}} \text{ s.t. } P \in S\}| \quad (3)$$

The *relative support* of P in \mathcal{D}_{SEQ} is the fraction

$$\text{rel-supp}(P) = \text{supp}(P) / |\mathcal{D}_{\text{SEQ}}| \quad (4)$$

Definition 3.15 (Confidence of a pair of events) The *confidence* of a pair of temporal events (E_i, E_j) in \mathcal{D}_{SEQ} is defined as

$$\text{conf}(E_i, E_j) = \frac{\text{supp}(E_i, E_j)}{\max\{\text{supp}(E_i), \text{supp}(E_j)\}} \quad (5)$$

Definition 3.16 (Confidence of a temporal pattern) The *confidence* of a temporal pattern P in \mathcal{D}_{SEQ} is defined as

$$\text{conf}(P) = \frac{\text{supp}(P)}{\max_{1 \leq k \leq |P|} \{\text{supp}(E_k)\}} \quad (6)$$

where $E_k \in P$ is a temporal event.

The denominator in Eq. (6) is the maximum support of the events in P . Thus, the confidence computed in Eq. (6) is the minimum confidence of a pattern P in \mathcal{D}_{SEQ} , representing how likely a pattern P (at least) is, given the occurrence of its most frequent event.

Problem Definition: Frequent Temporal Pattern Mining from Time Series (FTPMfTS). Given a set of time series $\mathcal{X} = \{X_1, \dots, X_n\}$, let \mathcal{D}_{SEQ} be the temporal sequence database obtained from \mathcal{X} , and σ and δ be the support and confidence thresholds, respectively. The FTPMfTS problem aims to find all temporal patterns P that have high enough support and confidence in \mathcal{D}_{SEQ} : $\text{supp}(P) \geq \sigma \wedge \text{conf}(P) \geq \delta$.

IV. FREQUENT TEMPORAL PATTERN MINING

A. Overview of the FTPMfTS Process

Fig. 2 depicts the overview of the FTPMfTS process to mine frequent patterns from a set of time series which consists of two phases. The first phase, *Data Transformation*, receives a set of time series \mathcal{X} as an input, and converts \mathcal{X} into a symbolic database \mathcal{D}_{SYB} through the *Symbolic Time Series Representation*. Then, \mathcal{D}_{SYB} is converted into a temporal sequence database \mathcal{D}_{SEQ} through the *Temporal Sequence Database Conversion*. The second phase, *Frequent Temporal Pattern Mining*, mines frequent patterns from \mathcal{D}_{SEQ} . This goes through three steps: (1) *Frequent Single Event Mining*, (2) *Frequent 2-Event Pattern Mining*, and (3) *Frequent k-Event Pattern Mining* ($k > 2$). The final output is a set of all frequent temporal patterns in \mathcal{D}_{SEQ} .

B. Data Transformation

1) *Symbolic Time Series Representation*: Given a set of time series \mathcal{X} , the symbolic representation of each time series $X \in \mathcal{X}$ can be easily obtained by using a mapping function described in Def. 3.2, after which will form \mathcal{D}_{SYB} .

2) *Temporal Sequence Database Conversion*: To convert \mathcal{D}_{SYB} to \mathcal{D}_{SEQ} , a straightforward approach is to split the symbolic time series in \mathcal{D}_{SYB} into equal length sequences, where each sequence belongs to one row in \mathcal{D}_{SEQ} . For example,

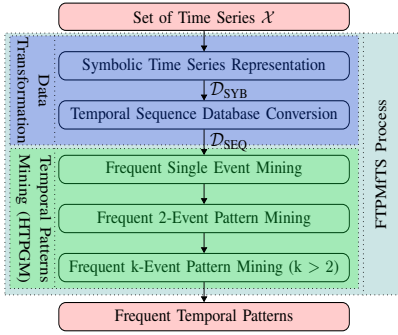


Fig. 2: The FTPMfTS process

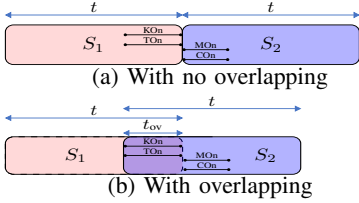


Fig. 3: Splitting strategy

consider Table I. If we decide to split each symbolic series in \mathcal{D}_{SYB} into 4 equal length sequences, then each sequence will last for 40 minutes. The first sequence S_1 of \mathcal{D}_{SEQ} therefore will contain temporal events of K, T, M, C, I, and B from 10:00 to 10:40. The second sequence S_2 contains temporal events from 10:45 to 11:25. Similarly for S_3 and S_4 .

However, the splitting can lead to a potential loss of temporal patterns. The loss happens when a *splitting point* accidentally divides a temporal pattern into different sub-patterns, and places them into separate sequences. We explain this situation in Fig. 3a, considering the two sequences S_1 and S_2 , each of length t . Here, the splitting point divides a pattern of 4 events, $\{K_{\text{On}}, T_{\text{On}}, M_{\text{On}}, C_{\text{On}}\}$, into two sub-patterns, in which K_{On} and T_{On} are placed in S_1 , and M_{On} and C_{On} in S_2 . This results in the loss of this 4-event pattern which can be identified only when all 4 events are in the same sequence.

To prevent the loss, we propose a *splitting strategy* using overlapping sequences. Specifically, two consecutive sequences are overlapped by a duration t_{ov} ($0 \leq t_{\text{ov}} \leq t_{\text{max}}$, where t_{max} is the *maximal duration* of a temporal pattern). The value of t_{ov} decides how large the overlap between S_i and S_{i+1} is: $t_{\text{ov}} = 0$ results in no overlap, i.e., no redundancy, but with a potential loss of patterns, while $t_{\text{ov}} = t_{\text{max}}$ creates large overlappings between sequences, i.e., high redundancy, but all patterns can be preserved. As illustrated in Fig. 3b, the overlapping between S_1 and S_2 keeps the 4 events together in the same sequence S_2 , and thus, helps preserve the pattern.

C. Frequent Temporal Patterns Mining

We now present our efficient mining method, called Hierarchical Temporal Pattern Graph Mining (HTPGM), to mine frequent temporal patterns from \mathcal{D}_{SEQ} . The main novelties of HTPGM lie in: a) the use of efficient data structures, i.e., the Hierarchical Pattern Graph and *bitmap indexing*, to enable fast computations for support and confidence, and b) the proposal of two groups of pruning techniques which are based on the Apriori principle and the temporal transitivity property of

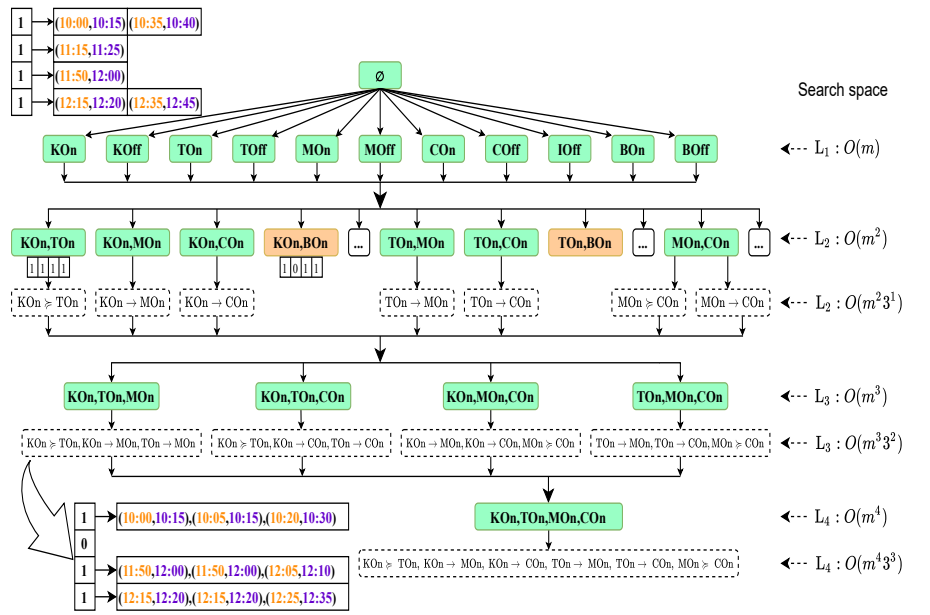


Fig. 4: A Hierarchical Pattern Graph for Table III

temporal events. Later in Section V, we introduce an additional pruning technique based on mutual information and is built on top of HTPGM to further optimize the mining process. We now discuss the efficient data structures used in our method.

Hierarchical Pattern Graph (HPG): We use a hierarchical graph structure, called the *Hierarchical Pattern Graph*, to keep track of the frequent events and patterns found in each mining step. This graph structure allows HTPGM to mine iteratively (e.g., 2-event patterns are mined based on frequent single events, 3-event patterns are mined based on 2-event patterns, and so on), and to do effective pruning. Fig. 4 shows the HPG built from \mathcal{D}_{SEQ} in Table III. The root of the graph is an empty set \emptyset , and each level L_k maintains frequent k -event patterns. As HTPGM proceeds, HPG is constructed gradually. We will explain this process in each of the following step.

Efficient bitmap indexing: We use *bitmap* to index the occurrences of events and patterns in \mathcal{D}_{SEQ} , enabling fast computations for support and confidence. Specifically, each event E or pattern P found in \mathcal{D}_{SEQ} is associated with a *bitmap* that indicates where E or P has occurred. Each *bitmap* b has length $|\mathcal{D}_{\text{SEQ}}|$ (i.e., the number of sequences), and has value $b[i] = 1$ if E or P is present in sequence i of \mathcal{D}_{SEQ} , or $b[i] = 0$ otherwise. Constructing the *bitmap* is also done step by step. For single events in \mathcal{D}_{SEQ} , *bitmaps* are built by scanning \mathcal{D}_{SEQ} only once. An example of *bitmap* can be seen at level L_1 in Fig. 4. The event K_{On} has the *bitmap* $b_{K_{\text{On}}} = [1, 1, 1, 1]$, indicating that K_{On} occurs in all sequences of \mathcal{D}_{SEQ} .

Algorithm 1 provides the pseudo code of HTPGM, which will be explained in details following each mining step.

D. Mining Frequent Single Events

The first step in HTPGM is to find frequent single events (Alg. 1, lines 1-4). This can easily be done using the *bitmap*. For each event E_i in \mathcal{D}_{SEQ} , the support $\text{supp}(E_i)$ is computed by counting the number of set bits in *bitmap* b_{E_i} , and comparing $\text{supp}(E_i)$ to the threshold σ . Note that for single events, *confidence* is not considered since it is always 1.

Algorithm 1: Hierarchical Temporal Pattern Graph Mining

Input: Temporal sequence database \mathcal{D}_{SEQ} , a support threshold σ , a confidence threshold δ

Output: The set of frequent temporal patterns P

// Mining frequent single events

```

1: foreach event  $E_i \in \mathcal{D}_{SEQ}$  do
2:    $supp(E_i) \leftarrow \text{countBitmap}(b_{E_i});$ 
3:   if  $supp(E_i) \geq \sigma$  then
4:     | Insert  $E_i$  to  $IFreq$ ;
// Mining frequent 2-event patterns
5: EventPairs  $\leftarrow \text{Cartesian}(IFreq, IFreq);$ 
6: FrequentPairs  $\leftarrow \emptyset;$ 
7: foreach  $(E_i, E_j)$  in EventPairs do
8:    $b_{ij} \leftarrow \text{AND}(b_{E_i}, b_{E_j});$ 
9:    $supp(E_i, E_j) \leftarrow \text{countBitmap}(b_{ij});$ 
10:  if  $supp(E_i, E_j) \geq \sigma$  then
11:    | FrequentPairs  $\leftarrow \text{Apply\_Lemma3}(E_i, E_j);$ 
12: foreach  $(E_i, E_j)$  in FrequentPairs do
13:  | Retrieve event instances;
14:  | Check frequent relations;
// Mining frequent k-event patterns
15: FilteredIFreq  $\leftarrow \text{Transitivity\_Filtering}(IFreq);$  //Lemmas 4,
    5
16: kEventCombinations  $\leftarrow \text{Cartesian}(\text{FilteredIFreq}, (k-1)\text{Freq});$ 
17: FrequentkEvents  $\leftarrow \text{Apriori\_Filtering}(k\text{EventCombinations});$ 
18: foreach  $k\text{Events}$  in FrequentkEvents do
19:  | Retrieve relations;
20:  | Iteratively check frequent relations; //Lemmas 4,
    6, 7

```

After this step, the set $IFreq$ containing frequent single events is created to build level L_1 of HPG. We illustrate this process using Table III, with $\sigma = 0.7$ and $\delta = 0.7$. Here, $IFreq$ contains 11 frequent events, each belongs to one node in L_1 . The event IOn is not frequent since it only appears in sequences 2 and 4, thus is omitted from L_1 . The data structure of each L_1 node contains a unique event name, a *bitmap*, and a list of event instances (see KOn at L_1 in Fig. 4).

Complexity: The complexity of finding frequent events is $O(m \cdot |\mathcal{D}_{SEQ}|)$, where m is the number of distinct events.

Proof. Detailed proofs of all complexities, lemmas and theorems in this article can be found in technical report [17].

E. Mining Frequent 2-event Patterns

1) *Search space of HTPGM:* The second step in HTPGM is to find frequent 2-event temporal patterns. A straightforward approach would be to enumerate all possible pairs of events, and check whether each event pair can form frequent patterns. However, this *naive* approach is very expensive. Not only does it need to repeatedly scan \mathcal{D}_{SEQ} to check each combination of events, the complex relations between events also result in an exponential growth of possible candidates, creating a very large search space that makes the approach infeasible.

Lemma 1. *Let m be the number of distinct events in \mathcal{D}_{SEQ} , and h be the longest length of a temporal pattern. The total number of temporal patterns in HPG from L_1 to L_h is $O(m^h 3^{h^2})$.*

2) *Two-steps filtering approach:* Given the huge set of candidates, it is prohibitively expensive to check their support

and confidence. To tackle this problem, we propose a *filtering approach* to reduce unnecessary candidate checking. More specifically, at any level h ($h \geq 2$) in HPG, the mining process is divided into two steps: (1) first, it finds only frequent nodes (i.e., remove infrequent combinations of events), (2) second, it generates temporal patterns only from frequent nodes found in the first step. The correctness of this filtering approach is based on the following Apriori-inspired lemmas.

Lemma 2. *Let (E_i, E_j) be a pair of events occurs in a 2-event pattern P . Then, $supp(P) \leq supp(E_i, E_j)$.*

Lemma 2 says that the support of a pattern is always at most the support of its events. Thus, if an event pair does not satisfy σ , it cannot occur in any frequent 2-event patterns.

Lemma 3. *Let (E_i, E_j) be a pair of events occurs in a 2-event pattern P . Then $conf(P) \leq conf(E_i, E_j)$.*

From Lemma 3, the confidence of a pattern P is always at most the confidence of its events. Thus, if an event pair does not satisfy δ , it cannot occur in any high confident patterns.

Applying Lemmas 2 and 3 to the first filtering step will remove infrequent or low confident event pairs. This helps reduce the pattern candidates while still ensuring the completeness of HTPGM. We detail the filtering approach below.

Step 2.1. Mining frequent pairs of events: This step finds frequent event pairs in \mathcal{D}_{SEQ} , using the set $IFreq$ found in L_1 of HPG (Alg. 1, lines 5-11). First, HTPGM generates all possible event pairs by calculating the Cartesian product $IFreq \times IFreq$. Next, for each pair (E_i, E_j) , the joint *bitmap* b_{ij} is computed by *ANDing* the two individual bitmaps: $b_{ij} = \text{AND}(b_{E_i}, b_{E_j})$ (b_{ij} represents the set of sequences where both events occur). Finally, HTPGM computes the support $supp(E_i, E_j)$ by counting the set bits in b_{ij} , and compares it against σ . Assume that $supp(E_i, E_j) \geq \sigma$, thus (E_i, E_j) has high enough support. We continue filtering (E_i, E_j) by applying Lemma 3: (E_i, E_j) is selected only if its confidence is at least δ . After this filtering step, only frequent and high confident event pairs remain and form the nodes in L_2 .

Step 2.2. Mining frequent 2-event patterns: This step finds frequent 2-event patterns from the nodes in L_2 (Alg. 1, lines 12-14). For each node $(E_i, E_j) \in L_2$, we use the *bitmap* b_{ij} to retrieve the set of sequences \mathcal{S} where both events are present. Next, for each sequence $S \in \mathcal{S}$, the pairs of event instances (e_i, e_j) are extracted, and the relations between them are verified. The support and confidence of each relation $r(E_{i \triangleright e_i}, E_{j \triangleright e_j})$ are computed and compared against the thresholds, after which only frequent relations are selected and stored in the corresponding node in L_2 . Examples of the relations in L_2 can be seen in Fig. 4, e.g., node (KOn, TOn).

The step 2.2 results in two different sets of nodes in L_2 . The first set contains nodes that are frequent but do not have any frequent patterns. These nodes (colored in brown in Fig. 4) are removed from L_2 . The second set are frequent nodes that also contain frequent patterns (colored in green), which remain in L_2 and are used in the subsequent mining steps.

Complexity: Let m be the number of frequent single events in L_1 , and i be the average number of event instances of each

frequent event. The complexity of frequent 2-event pattern mining is $O(m^2 i^2 |\mathcal{D}_{\text{SEQ}}|^2)$.

F. Mining Frequent k -event Patterns

Mining frequent k -event patterns ($k \geq 3$) follows a similar process as 2-event patterns, with additional prunings based on the transitivity property of temporal relations.

Step 3.1 Mining frequent k -event combinations: to find frequent k -event combinations in L_k (Alg. 1, lines 15-17).

Let $(k-1)\text{Freq}$ be the set of frequent $(k-1)$ -event combinations found in L_{k-1} , and 1Freq be the set of frequent single events in L_1 . To generate all k -event combinations, the usual process is to compute the Cartesian product: $(k-1)\text{Freq} \times 1\text{Freq}$. However, we observe that using 1Freq to generate event combinations at L_k can create redundancy, since 1Freq might contain events that when combining with nodes in L_{k-1} , result in combinations that clearly cannot have any frequent patterns. To illustrate this observation, consider node BOn at L_1 in Fig. 4. Here, BOn is a frequent event, and thus, can be combined with frequent nodes in L_2 such as (KOn, TOn) to create a 3-event combination (KOn, TOn, BOn). However, (KOn, TOn, BOn) cannot form any frequent 3-event patterns, since BOn is not present in any frequent 2-event patterns in L_2 . To reduce the redundancy, the combination (KOn, TOn, BOn) should not be created in the first place. We rely on the *transitivity property* of temporal relations to identify such event combinations.

Lemma 4. Let $S = \langle e_1, \dots, e_{n-1} \rangle$ be a temporal sequence that supports an $(n-1)$ -event pattern $P = \langle (E_{1 \triangleright e_1}, r_{12}, E_{2 \triangleright e_2}), \dots, (E_{n-2 \triangleright e_{n-2}}, r_{(n-2)(n-1)}, E_{n-1 \triangleright e_{n-1}}) \rangle$.

Let e_n be a new event instance that is added to S to create a temporal sequence $S' = \langle e_1, \dots, e_n \rangle$. Then the set of temporal relations \mathfrak{R} is transitive on S' : $\forall e_i \in S', i \neq n, \exists r \in \mathfrak{R}$ s.t. $r(E_{i \triangleright e_i}, E_{n \triangleright e_n})$ holds.

Lemma 4 says that, a new event instance can always form temporal relations with existing instances of an existing temporal sequence. Based on this transitivity property, we can prove the following lemma.

Lemma 5. Let $N_{k-1} = (E_1, \dots, E_{k-1})$ be a frequent combination of $(k-1)$ events, and E_k be a frequent single event. The combination $N_k = N_{k-1} \cup E_k$ cannot form any frequent k -event temporal patterns if $\nexists E_i \in N_{k-1}, r \in \mathfrak{R}$ s.t. $r(E_i, E_k)$ is a frequent temporal relation.

From Lemma 5, only single events in L_1 that form at least one frequent pattern in L_{k-1} should be used to create event combinations in L_k . Using this result, we perform an initial filtering on 1Freq ahead of the Cartesian product calculation. Specifically, from the nodes in L_{k-1} , we extract the distinct single events D_{k-1} , and intersect them with 1Freq to remove redundant single events: $\text{Filtered}1\text{Freq} = D_{k-1} \cap 1\text{Freq}$. Then, the Cartesian product $(k-1)\text{Freq} \times \text{Filtered}1\text{Freq}$ is calculated to generate all possible k -event combinations. Next, we apply Lemmas 2 and 3 to select only frequent and high confident k -event combinations $k\text{Freq}$ to form L_k .

Step 3.2 Mining frequent k -event patterns: This step finds frequent k -event patterns from the nodes in L_k (Alg. 1, lines 18-20). Unlike 2-event patterns, determining the relations

in a k -event combination ($k \geq 3$) is much more expensive, as it requires to verify the frequency of $\frac{1}{2}k(k-1)$ triples. To reduce the cost of relation checking, we propose an iterative verification approach that also relies on the *transitivity property* of temporal relations.

Lemma 6. Let P and P' be two temporal patterns. If $P' \subseteq P$, then $\text{conf}(P') \geq \text{conf}(P)$.

Lemma 7. Let P and P' be two temporal patterns. If $P' \subseteq P$ and $\frac{\text{supp}(P')}{\max_{1 \leq k \leq |P'|} \{\text{supp}(E_k)\}_{E_k \in P'}} \leq \delta$, then $\text{conf}(P) \leq \delta$.

Lemmas 6, 7 say that a temporal pattern P cannot be high confident if any of its sub-patterns has low confidence.

Let $N_{k-1} = (E_1, \dots, E_{k-1})$ be a node in L_{k-1} , $N_1 = (E_k)$ be a node in L_1 , and $N_k = N_{k-1} \cup N_1 = (E_1, \dots, E_k)$ be a node in L_k . To find k -event patterns for N_k , we first retrieve the set P_{k-1} containing frequent $(k-1)$ -event patterns in node N_{k-1} . Each $p_{k-1} \in P_{k-1}$ is a list of $\frac{1}{2}(k-1)(k-2)$ triples: $\{(E_{1 \triangleright e_1}, r_{12}, E_{2 \triangleright e_2}), \dots, (E_{k-2 \triangleright e_{k-2}}, r_{(k-2)(k-1)}, E_{k-1 \triangleright e_{k-1}})\}$. We iteratively verify the possibility of p_{k-1} forming a frequent k -event pattern with E_k as follows.

We first check whether the triple $(E_{k-1 \triangleright e_{k-1}}, r_{(k-1)k}, E_{k \triangleright e_k})$ is frequent and high confident by accessing the node (E_{k-1}, E_k) in L_2 . If the triple is not frequent (using Lemmas 4 and 5) or high confident (using Lemmas 4, 6, and 7), the verifying process stops immediately for p_{k-1} . Otherwise, it continues on the triple $(E_{k-2 \triangleright e_{k-2}}, r_{(k-2)k}, E_{k \triangleright e_k})$, until it reaches $(E_{1 \triangleright e_1}, r_{1k}, E_{k \triangleright e_k})$.

Complexity: Let r be the average number of frequent $(k-1)$ -event patterns in L_{k-1} . The complexity of frequent k -event pattern mining is $O(|1\text{Freq}| \cdot |L_{k-1}| \cdot r \cdot k^2 \cdot |\mathcal{D}_{\text{SEQ}}|)$.

V. APPROXIMATE HTPGM USING MUTUAL INFORMATION

In this section, we first use mutual information (MI) to derive the lower bound of confidence for an event pair, and show that frequent temporal patterns extracted from *correlated* symbolic time series have confidences above this bound. Based on this result, we propose an approximation for HTPGM that mines frequent temporal patterns only from the \mathcal{D}_{SYB} subset of *correlated* symbolic time series, and thus, significantly reduces the search space. Our experiments in Section VI also show that temporal patterns extracted from *uncorrelated* time series are typically infrequent and have low confidence, thus are generally not interesting to explore.

A. Correlated Symbolic Time Series

Definition 5.1 (Entropy) The *entropy* of a symbolic time series \mathcal{X}_S , denoted as $H(\mathcal{X}_S)$, is defined as

$$H(\mathcal{X}_S) = - \sum_{x \in \Sigma_X} p(x) \cdot \log p(x) \quad (7)$$

where Σ_X is the symbolic alphabet of \mathcal{X}_S . Intuitively, the entropy measures the amount of information or uncertainty inherent in the possible outcomes of a random variable. The higher the $H(\mathcal{X}_S)$, the more uncertain the outcome of \mathcal{X}_S .

The conditional entropy $H(\mathcal{X}_S | \mathcal{Y}_S)$ quantifies the amount of information needed to describe the outcome of \mathcal{X}_S , given the value of \mathcal{Y}_S , and is defined as

$$H(\mathcal{X}_S | \mathcal{Y}_S) = - \sum_{x \in \Sigma_X} \sum_{y \in \Sigma_Y} p(x, y) \cdot \log \frac{p(x, y)}{p(y)} \quad (8)$$

Definition 5.2 (Mutual information) The *mutual information* of two symbolic time series \mathcal{X}_S and \mathcal{Y}_S , denoted as $I(\mathcal{X}_S; \mathcal{Y}_S)$, is defined as

$$I(\mathcal{X}_S; \mathcal{Y}_S) = \sum_{x \in \Sigma_X} \sum_{y \in \Sigma_Y} p(x, y) \cdot \log \frac{p(x, y)}{p(x) \cdot p(y)} \quad (9)$$

The mutual information represents the reduction of uncertainty of one variable (e.g., \mathcal{X}_S), given the knowledge of another variable (e.g., \mathcal{Y}_S). The larger $I(\mathcal{X}_S; \mathcal{Y}_S)$, the more information is shared between \mathcal{X}_S and \mathcal{Y}_S , and thus, the less uncertainty about one variable when knowing the other.

We demonstrate how to compute the MI between the symbolic series K and T in Table I. We have: $p(\text{KOn}) = \frac{17}{36}$, $p(\text{KOff}) = \frac{19}{36}$, $p(\text{TON}) = \frac{18}{36}$, and $p(\text{TOff}) = \frac{18}{36}$. We also have: $p(\text{KOn, TOn}) = \frac{15}{36}$, $p(\text{KOff, TOff}) = \frac{16}{36}$, $p(\text{KOn, TOff}) = \frac{2}{36}$, and $p(\text{KOff, TOn}) = \frac{3}{36}$. Using Eq. 9, we have $I(K; T) = 0.29$.

Since $0 \leq I(\mathcal{X}_S; \mathcal{Y}_S) \leq \min(H(\mathcal{X}_S), H(\mathcal{Y}_S))$ [18], the upper bound of MI values is unbounded. To scale the MI value into the range $[0 - 1]$, we use normalized mutual information as defined below.

Definition 5.3 (Normalized mutual information) The *normalized mutual information* (NMI) of two symbolic time series \mathcal{X}_S and \mathcal{Y}_S , denoted as $\tilde{I}(\mathcal{X}_S; \mathcal{Y}_S)$, is defined as

$$\tilde{I}(\mathcal{X}_S; \mathcal{Y}_S) = \frac{I(\mathcal{X}_S; \mathcal{Y}_S)}{H(\mathcal{X}_S)} = 1 - \frac{H(\mathcal{X}_S | \mathcal{Y}_S)}{H(\mathcal{X}_S)} \quad (10)$$

$\tilde{I}(\mathcal{X}_S; \mathcal{Y}_S)$ represents the percentage of reduction of uncertainty about \mathcal{X}_S due to knowing \mathcal{Y}_S . Based on Eq. 10, any pair of variables $(\mathcal{X}_S, \mathcal{Y}_S)$ that has $\tilde{I}(\mathcal{X}_S; \mathcal{Y}_S) > 0$ will have a certain mutual dependency. Eq. 10 also shows that NMI is not symmetric, i.e., $\tilde{I}(\mathcal{X}_S; \mathcal{Y}_S) \neq \tilde{I}(\mathcal{Y}_S; \mathcal{X}_S)$.

Using Table I, we have $I(K; T) = 0.29$. However, we do not know what the 0.29 reduction means in practice. Using NMI in Eq. 10, we have $\tilde{I}(K; T) = 0.43$, which says that the uncertainty of K is reduced by 43% given T . Moreover, we have $\tilde{I}(T; K) = 0.42$, showing that $\tilde{I}(K; T) \neq \tilde{I}(T; K)$.

Definition 5.4 (Correlated symbolic time series) Let μ ($0 < \mu \leq 1$) be the mutual information threshold, and \mathcal{X}_S and \mathcal{Y}_S be the symbolic time series. We say that \mathcal{X}_S and \mathcal{Y}_S are *correlated* iff $\tilde{I}(\mathcal{X}_S; \mathcal{Y}_S) \geq \mu$, and *uncorrelated* otherwise.

B. Lower Bound of the Confidence

Consider two time series X and Y , and their corresponding symbolic series \mathcal{X}_S and \mathcal{Y}_S . Let X_1 be a temporal event in X , Y_1 be a temporal event in Y , and \mathcal{D}_{SYB} , \mathcal{D}_{SEQ} be the symbolic database and the temporal sequence database created from \mathcal{X}_S and \mathcal{Y}_S , respectively. We first study the relationship between the supports of (X_1, Y_1) in \mathcal{D}_{SYB} and \mathcal{D}_{SEQ} .

Lemma 8. Let $\text{supp}(X_1, Y_1)_{\mathcal{D}_{\text{SYB}}}$ and $\text{supp}(X_1, Y_1)_{\mathcal{D}_{\text{SEQ}}}$ be the supports of (X_1, Y_1) in \mathcal{D}_{SYB} and \mathcal{D}_{SEQ} , respectively. We have: $\text{supp}(X_1, Y_1)_{\mathcal{D}_{\text{SYB}}} \leq \text{supp}(X_1, Y_1)_{\mathcal{D}_{\text{SEQ}}}$.

Lemma 8 says that, if an event pair is frequent in \mathcal{D}_{SYB} , it is also frequent in \mathcal{D}_{SEQ} . We now investigate the connection between the NMI of \mathcal{X}_S and \mathcal{Y}_S in \mathcal{D}_{SYB} , i.e., $\tilde{I}(\mathcal{X}_S; \mathcal{Y}_S)$, and the confidence of the event pair (X_1, Y_1) in \mathcal{D}_{SEQ} below.

Theorem 1. (Confidence lower bound) Let σ and μ be the support and the mutual information thresholds, respectively. Assume that (X_1, Y_1) is frequent in \mathcal{D}_{SYB} ,

i.e., $\text{supp}(X_1, Y_1)_{\mathcal{D}_{\text{SYB}}} \geq \sigma$. If $\tilde{I}(\mathcal{X}_S; \mathcal{Y}_S) \geq \mu$, then $\text{conf}(X_1, Y_1)_{\mathcal{D}_{\text{SEQ}}} \geq \text{LB}$ where

$$\text{LB} = \left(\sigma^{\sigma_m} \cdot \left(\frac{1 - \sigma_m}{n_x - 1} \right)^{1 - \sigma} \right)^{\frac{1 - \mu}{\sigma}} \cdot \frac{\sigma}{2 \cdot \sigma_m - \sigma} \quad (11)$$

where n_x is the number of symbols in the symbol alphabet Σ_X , and σ_m be the maximum support of (X_1, Y_1) in \mathcal{D}_{SYB} .

From Theorem 1, if X_S and Y_S are correlated w.r.t. μ , then the confidence of a frequent event pair is at least the lower bound LB (Eq. (11)) in \mathcal{D}_{SEQ} . Combining Theorem 1 and Lemma 3, we can say that if an event pair has a confidence less than LB, then any pattern P containing that event pair also has a confidence less than LB. Next, based on this result, we propose an approximation for HTPGM.

C. Approximate HTPGM using the Confidence Lower Bound

Using Theorem 1, HTPGM can be approximated by first finding the set of correlated symbolic series $\mathcal{X}_C \subseteq \mathcal{X}$, and then performing the mining only on \mathcal{X}_C . To explain how HTPGM can mine using \mathcal{X}_C , we first define the correlation graph.

Definition 5.5 (Correlation graph) A *correlation graph* is an *undirected* graph $G_C = (V, E)$ where V is the set of vertices, and E is the set of edges. Each vertex $v_i \in V$ represents one symbolic series $\mathcal{X}_i \in \mathcal{X}_C$. There is an edge e_{ij} between a vertex v_i containing \mathcal{X}_i , and a vertex v_j containing \mathcal{X}_j iff $\tilde{I}(\mathcal{X}_i; \mathcal{X}_j) \geq \mu \wedge \tilde{I}(\mathcal{X}_j; \mathcal{X}_i) \geq \mu$.

Since NMI is not symmetric, in a correlation graph, there is an edge between two vertices only if their NMIs satisfy μ in both directions. Thus, the correlation graph is undirected.

Setting the value of μ : We propose to rely on the density of the correlation graph to set the value of μ .

Definition 5.6 (Correlation graph density) Consider a correlation graph $G_C = (V, E)$. Let \mathcal{G} be the complete graph of G_C . The *correlation graph density* d_C is the ratio between the number of edges in G_C and the number of edges in \mathcal{G} .

The value of d_C represents the density of G_C w.r.t. \mathcal{G} . Intuitively, given μ , G_C is the graph obtained after pruning \mathcal{G} (by removing edges that do not satisfy μ). Therefore, using the correlation graph density, we can choose μ such that it satisfies a given expected density $\mathbb{E}(d_C)$. The higher d_C , the more edges remained in \mathcal{G} (the fewer edges pruned from \mathcal{G}).

As an example, consider \mathcal{D}_{SYB} in Table I which has 6 symbolic series. The complete graph of 6 vertices (each corresponds to one symbolic series) has 15 edges. If we set the density of the correlation graph to be 40%, then G_C will have: $15 \times 40\% = 6$ edges, which corresponds to $\mu = 0.40$. Fig. 5 shows an example of G_C built from \mathcal{D}_{SYB} in Table I.

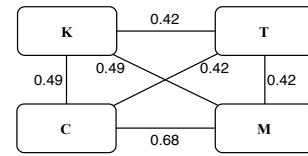


Fig. 5: Correlation graph

Algorithm 2 illustrates how HTPGM can be approximated using the correlation graph G_C . First, to find the set \mathcal{X}_C , we

compute NMI for each pair of symbolic series $(\mathcal{X}_S, \mathcal{Y}_S)$ in \mathcal{D}_{SYB} (line 3). Next, only pairs where both $\tilde{I}(\mathcal{X}_S; \mathcal{Y}_S)$ and $\tilde{I}(\mathcal{Y}_S; \mathcal{X}_S)$ of at least μ are inserted into \mathcal{X}_C (lines 4-5), and an edge between \mathcal{X}_S and \mathcal{Y}_S is created in G_C (line 6). Next, at L_1 of HPG, only the correlated symbolic series present in \mathcal{X}_C are used to generate single events (lines 7-8). At L_2 , G_C is used to filter 2-event combinations, adding an additional filtering step to HTPGM as follows. For each event pair (E_i, E_j) , we check whether there is an edge between the symbolic series of E_i and of E_j in G_C . If so, we proceed by computing the support and confidence of (E_i, E_j) as in the exact HTPGM (lines 9-11). Otherwise, (E_i, E_j) is eliminated from the mining of L_2 . From level L_k ($k \geq 3$) onwards, the mining is the same as for the exact HTPGM (lines 12-13).

Algorithm 2: Approximate HTPGM using MI

Input: A set of time series \mathcal{X} , an MI threshold μ , support threshold σ , confidence threshold δ
Output: The set of frequent temporal patterns P

- 1: convert \mathcal{X} to \mathcal{D}_{SYB} and \mathcal{D}_{SEQ} ;
- 2: **foreach** pair of symbolic time series $(\mathcal{X}_S, \mathcal{Y}_S) \in \mathcal{D}_{\text{SYB}}$ **do**
- 3: compute $\tilde{I}(\mathcal{X}_S; \mathcal{Y}_S)$ and $\tilde{I}(\mathcal{Y}_S; \mathcal{X}_S)$;
- 4: **if** $\tilde{I}(\mathcal{X}_S; \mathcal{Y}_S) \geq \mu \wedge \tilde{I}(\mathcal{Y}_S; \mathcal{X}_S) \geq \mu$ **then**
- 5: insert \mathcal{X}_S and \mathcal{Y}_S into \mathcal{X}_C ;
- 6: create an edge between \mathcal{X}_S and \mathcal{Y}_S in G_C ;
- 7: **foreach** $\mathcal{X}_i \in \mathcal{X}_C$ **do**
- 8: | Mine frequent single events from \mathcal{X}_i ;
- 9: **foreach** event pair (E_i, E_j) **do**
- 10: | **if** There is an edge between \mathcal{X}_i and \mathcal{X}_j in G_C **then**
- 11: | Mine frequent patterns for (E_i, E_j) ;
- 12: **if** $k \geq 3$ **then**
- 13: | Perform HTPGM using L_1 and L_2 ;

Complexity analysis: To compute the NMI, we only have to scan \mathcal{D}_{SYB} once to compute the probability of each individual event. Thus, the complexity of NMI computation is $|\mathcal{D}_{\text{SYB}}|$. On the other hand, the complexity to mine frequent 2-event patterns in the exact HTPGM is $O(m^2 i^2 |\mathcal{D}_{\text{SEQ}}|^2)$ (Section IV-E). Thus, we can expect that the approximate HTPGM using MI can significantly improve the performance of HTPGM.

VI. EXPERIMENTAL EVALUATION

We evaluate HTPGM (both exact and approximate), using real-world datasets from two application domains: smart energy and smart city. The evaluation is both qualitative (to assess the quality of extracted patterns) and quantitative (to evaluate the scalability and efficiency of HTPGM).

A. Experimental Setup

1) *Datasets:* We use 3 smart energy datasets: NIST [19], UKDALE [20], and DataPort [21], all of which measure the energy/power consumption of electrical appliances in residential households. For the smart city datasets, we use weather and vehicle collision datasets obtained from NYC Open Data Portal [22]. The datasets contain information about weather conditions, and the collision incidents in New York City. Table IV summarizes the characteristics of each dataset.

TABLE IV: Characteristics of the Datasets

| | NIST [19] | UKDALE [20] | DataPort [21] | Smart City [22] |
|------------------------------|-----------|-------------|---------------|-----------------|
| # of sequences | 1460 | 1520 | 1210 | 1216 |
| # of variables | 72 | 53 | 21 | 59 |
| # of distinct events | 144 | 106 | 42 | 266 |
| Avg. # of instances/sequence | 140 | 126 | 163 | 155 |

2) *Obtaining symbolic representations:* Data collected from the energy and smart city datasets are numerical time series which need to be converted into symbolic representations. For the energy datasets, the symbol alphabet Σ contains only two symbols: On and Off. The threshold for an On symbol is $v_t \geq 0.05$, and Off otherwise (v_t is the time series value at time t).

Unlike the energy data, weather conditions and vehicle collisions have more than 2 states. For example, temperature can be classified into {Very Cold, Cold, Mild, Hot, Very Hot}, or the number of injuries can be categorized as {None, Low, Medium, High}. To define the mapping function between Σ and the time series values, we rely on the percentile distribution of data. The percentile values depend on the specific variables. For example, we use 10th, 25th, 50th, 75th, 95th percentiles for a variable that has 5 states.

3) *Baseline methods:* Our exact method is referred to as E-HTPGM, and the approximate one as A-HTPGM. We use 3 different baselines (description in Section II): (1) TPMiner [1], (2) IEMiner [2], and (3) H-DFS [3]. Since both E-HTPGM and the baselines provide the same exact solutions, we only use the baselines for quantitative evaluation, and compare qualitatively only between E-HTPGM and A-HTPGM.

4) *Infrastructure:* All methods, E-HTPGM, A-HTPGM and the baselines are implemented in Python. The experiments are run on a single machine with Intel Core i7-4770HQ (2.2GHz) CPU, 16 GB main memory.

B. Qualitative Evaluation

In this evaluation, our goal is to make sense and learn insights from extracted patterns. Due to space limitations, we show just a few of them below.

1) *Generated temporal patterns:* We first summarize in Table V the number of extracted patterns for each dataset. We can see that, the Smart City dataset generate more patterns than the energy datasets, since its variables have more states.

2) *Interpretation of extracted patterns:* Table VI summarizes some interesting patterns we found in the datasets, together with the support and confidence. Patterns P1 - P11 are extracted from the energy datasets, which show that through analyzing the interactions of the residents with electrical devices, we can understand their living patterns/habits. Patterns P12 - P17 show the association between weather conditions and the collision situations. Such patterns indicate that extreme or abnormal weather conditions are linked to a high number of collisions. Moreover, they occur with low support but high confidence, implying that such patterns are rare, but with strong confidence of the association.

C. Quantitative Evaluation

1) *Baselines comparison:* We compare E-HTPGM and A-HTPGM with the baselines in terms of runtimes and memory usage. A-HTPGM is run with 4 different values of μ (80%, 60%, 40%, 20%) which correspond to 80%, 60%, 40%, and

TABLE V: Summary of Extracted Patterns

| Support (%) | Confidence (%) | | | | | | | | | | | | | | | |
|-------------|----------------|---------|--------|--------|---------|--------|--------|-------|----------|---------|--------|-------|------------|-----------|---------|-------|
| | NIST | | | | UKDALE | | | | DataPort | | | | Smart City | | | |
| | 20 | 40 | 60 | 80 | 20 | 40 | 60 | 80 | 20 | 40 | 60 | 80 | 20 | 40 | 80 | |
| 20 | 519,316 | 378,896 | 69,951 | 28,912 | 126,490 | 39,629 | 10,562 | 4,231 | 310,713 | 200,179 | 11,074 | 5,012 | 1,201,723 | 1,001,354 | 121,140 | 7,164 |
| 40 | 96,952 | 96,952 | 46,793 | 14,193 | 46,193 | 26,172 | 8,240 | 4,129 | 201,561 | 140,984 | 8,928 | 4,813 | 91,241 | 90,198 | 76,014 | 6,891 |
| 60 | 29,955 | 29,955 | 29,955 | 9,608 | 11,247 | 6,221 | 5,392 | 3,921 | 9,781 | 7,229 | 6,582 | 3,827 | 13,126 | 8,712 | 6,286 | 6,140 |
| 80 | 3,568 | 3,568 | 3,568 | 3,568 | 4,832 | 4,321 | 3,251 | 3,251 | 5,492 | 4,825 | 3,981 | 3,370 | 7,018 | 6,872 | 6,002 | 6,002 |

TABLE VI: Summary of Interesting Patterns

| Patterns | Supp. % | Conf. % |
|--|---------|---------|
| (P1) ([05:58, 08:24] First Floor Lights On) \succ ([05:58, 06:59] Upstairs Bathroom Lights On) \succ ([05:59, 06:06] Microwave On) | 20 | 30 |
| (P2) ([06:00, 07:01] Upstairs Bathroom Lights On) \succ ([06:40, 06:46] Upstairs Bathroom Plugs On) | 30 | 20 |
| (P3) ([18:00, 18:30] Lights Dining Room On) \rightarrow ([18:31, 20:16] Children Room Plugs On) $\hat{=}$ ([19:00, 22:31] Lights Living Room On) | 20 | 20 |
| (P4) ([15:59, 16:05] Hallway Lights On) \rightarrow ([17:58, 18:29] Kitchen Lights On \succ ([18:00, 18:18] Plug In Kitchen On) \succ ([18:08, 18:15] Microwave On) | 80 | 60 |
| (P5) ([06:02, 06:19] Kitchen Lights On) \rightarrow ([06:05, 06:12] Microwave On) $\hat{=}$ ([06:09, 06:11] Kettle On) | 20 | 5 |
| (P6) ([05:58,08:24] First Floor Lights On) \succ ([05:58,06:59] Upstairs Bathroom Lights On) \succ ([05:59, 06:06] Microwave On) | 20 | 30 |
| (P7) ([06:00,07:01] Upstairs Bathroom Lights On) \succ ([06:40,06:46] Upstairs Bathroom Plugs On) | 30 | 20 |
| (P8) ([18:10,18:15] Kitchen App On) \rightarrow ([18:15,19:00] Lights Plugs On) \succ ([18:20,18:25] Microwave On) \rightarrow ([18:25,18:55] Cooktop On) \rightarrow ([19:30,20:20] Clothes Dryer On) | 5 | 50 |
| (P9) ([16:45, 17:30] Clothes Washer On) \rightarrow ([17:40,18:55] Clothes Dryer On) \rightarrow ([19:05, 20:10] Dining Room Lights On) \succ ([19:10, 19:30] Cooktop On) | 10 | 30 |
| (P10) ([06:10, 07:00] Kitchen Lights On) \succ ([06:10, 06:15] Kettle On) \rightarrow ([06:30, 06:40] Toaster On) \rightarrow ([06:45, 06:48] Microwave On) | 25 | 40 |
| (P11) ([18:00, 18:25] Kitchen Lights On) \succ ([18:00, 18:05] Kettle On) \rightarrow ([18:05, 18:10] Microwave On) \rightarrow ([19:35, 20:50] Washing Machine On) | 20 | 40 |
| (P12) ([13:10, 22:35] Heavy Rain) \succ ([14:00, 22:35] Unclear Visibility) \succ ([15:00, 20:55] Overcast Cloudiness) \rightarrow ([21:00, 21:55] High Motorist Injury) | 5 | 30 |
| (P13) ([19:00, 21:50] Unclear Extremely Visibility) \succ ([19:00, 21:50] High Snow) \succ ([20:00, 20:55] High Motorist Injury) | 30 | 45 |
| (P14) Very Strong Wind \rightarrow High Motorist Injury | 5 | 40 |
| (P15) Frost Temperature \rightarrow Medium Cyclist Injury | 5 | 20 |
| (P16) Strong Wind \rightarrow High Pedestrian Killed | 4 | 30 |
| (P17) Strong Wind \rightarrow High Motorist Killed | 4 | 10 |

TABLE VII: Runtime Comparison (seconds)

| Support (%) | Methods | Confidence (%) | | | | | |
|---------------|---------------|----------------|--------------|--------------|--------------|-------------|-------------|
| | | NIST | | | Smart City | | |
| | | 20 | 50 | 80 | 20 | 50 | 80 |
| 20 | H-DFS | 23391.83 | 319.17 | 87.11 | 2516.64 | 223.47 | 10.27 |
| | IEMiner | 21615.74 | 219.59 | 77.24 | 1419.51 | 130.80 | 8.59 |
| | TPMiner | 3919.40 | 214.96 | 67.30 | 418.25 | 118.89 | 6.66 |
| | E-HTPGM | 410.81 | 50.92 | 16.59 | 136.53 | 46.42 | 3.38 |
| | A-HTPGM (80%) | 173.43 | 35.85 | 15.81 | 78.69 | 29.02 | 3.05 |
| | A-HTPGM (60%) | 21.23 | 20.48 | 15.43 | 24.61 | 10.67 | 2.42 |
| | A-HTPGM (40%) | 20.74 | 19.98 | 14.43 | 21.70 | 9.54 | 2.19 |
| | A-HTPGM (20%) | 19.25 | 18.68 | 13.15 | 15.61 | 8.71 | 2.05 |
| | 50 | H-DFS | 830.17 | 190.06 | 83.62 | 453.47 | 88.32 |
| IEMiner | | 419.59 | 171.30 | 72.37 | 300.8 | 73.81 | 7.81 |
| TPMiner | | 214.96 | 144.05 | 62.78 | 118.89 | 37.54 | 6.14 |
| E-HTPGM | | 49.92 | 31.49 | 14.66 | 86.42 | 16.75 | 3.12 |
| A-HTPGM (80%) | | 22.12 | 21.09 | 13.52 | 12.34 | 12.30 | 2.84 |
| A-HTPGM (60%) | | 18.03 | 15.03 | 13.00 | 11.71 | 6.15 | 2.29 |
| A-HTPGM (40%) | | 17.83 | 14.07 | 12.65 | 6.34 | 6.11 | 2.19 |
| A-HTPGM (20%) | | 16.68 | 12.73 | 12.58 | 6.20 | 5.86 | 2.03 |
| 80 | | H-DFS | 157.11 | 68.39 | 59.35 | 13.27 | 8.39 |
| | IEMiner | 107.24 | 63.42 | 58.39 | 9.59 | 5.47 | 4.37 |
| | TPMiner | 57.30 | 55.02 | 50.73 | 6.66 | 3.44 | 3.37 |
| | E-HTPGM | 17.59 | 14.60 | 12.66 | 3.38 | 1.96 | 1.67 |
| | A-HTPGM (80%) | 16.74 | 13.78 | 11.88 | 2.50 | 1.52 | 1.49 |
| | A-HTPGM (60%) | 16.60 | 13.66 | 11.72 | 2.45 | 1.18 | 1.09 |
| | A-HTPGM (40%) | 14.66 | 12.63 | 11.19 | 2.15 | 1.15 | 1.06 |
| | A-HTPGM (20%) | 13.15 | 11.62 | 10.34 | 1.32 | 1.13 | 1.05 |

TABLE VIII: Memory Usage Comparison (MB)

| Support (%) | Methods | Confidence (%) | | | | | |
|---------------|---------------|----------------|---------------|---------------|---------------|---------------|--------------|
| | | NIST | | | Smart City | | |
| | | 20 | 50 | 80 | 20 | 50 | 80 |
| 20 | H-DFS | 3353.3 | 1519.13 | 796.45 | 1293.28 | 412.14 | 107.89 |
| | IEMiner | 2942.37 | 1015.79 | 675.51 | 1197.74 | 353.18 | 65.92 |
| | TPMiner | 2487.52 | 895.61 | 424.36 | 1002.82 | 254.26 | 61.23 |
| | E-HTPGM | 1870.45 | 356.58 | 185.41 | 807.41 | 167.85 | 46.13 |
| | A-HTPGM (80%) | 1250.22 | 316.67 | 174.09 | 594.90 | 145.39 | 43.36 |
| | A-HTPGM (60%) | 326.39 | 214.61 | 164.32 | 297.68 | 129.82 | 42.61 |
| | A-HTPGM (40%) | 248.52 | 208.40 | 161.69 | 265.84 | 129.24 | 41.89 |
| | A-HTPGM (20%) | 222.39 | 204.61 | 158.93 | 257.68 | 128.82 | 40.76 |
| | 50 | H-DFS | 2070.57 | 971.66 | 627.00 | 1040.56 | 470.49 |
| IEMiner | | 1867.60 | 890.14 | 591.58 | 870.64 | 460.52 | 60.87 |
| TPMiner | | 1078.42 | 671.18 | 502.83 | 660.66 | 150.68 | 58.98 |
| E-HTPGM | | 328.41 | 269.21 | 162.25 | 144.13 | 134.07 | 46.04 |
| A-HTPGM (80%) | | 262.34 | 263.25 | 162.09 | 142.59 | 127.49 | 43.15 |
| A-HTPGM (60%) | | 192.82 | 169.89 | 160.69 | 130.76 | 122.88 | 42.33 |
| A-HTPGM (40%) | | 171.99 | 168.36 | 150.04 | 122.36 | 121.23 | 41.36 |
| A-HTPGM (20%) | | 167.82 | 144.34 | 140.53 | 120.03 | 119.93 | 40.62 |
| 80 | | H-DFS | 794.19 | 589.09 | 549.88 | 249.78 | 139.59 |
| | IEMiner | 656.12 | 518.44 | 501.93 | 149.45 | 119.83 | 59.59 |
| | TPMiner | 486.57 | 482.34 | 476.74 | 119.59 | 69.91 | 58.63 |
| | E-HTPGM | 162.82 | 153.18 | 141.80 | 64.30 | 44.22 | 43.16 |
| | A-HTPGM (80%) | 160.63 | 152.23 | 141.00 | 60.74 | 41.68 | 39.72 |
| | A-HTPGM (60%) | 160.41 | 151.37 | 140.66 | 49.15 | 40.93 | 38.05 |
| | A-HTPGM (40%) | 156.34 | 145.96 | 136.98 | 46.59 | 39.64 | 36.82 |
| | A-HTPGM (20%) | 150.24 | 131.12 | 128.31 | 39.03 | 37.06 | 30.93 |

20% of the edges in the correlation graph. Tables VII and VIII show the results on the NIST and Smart City datasets.

It can be seen that E-HTPGM and A-HTPGM have better performance (both runtimes and memory usage) than the baselines, with A-HTPGM achieving the best performance among all methods. On the tested datasets, the range and average speedups of E-HTPGM compared to the baselines are: [1.3–9.5] and 3.69 (TPMiner), [2.8–53] and 12.12 (IEMiner), and [3.9–56.9] and 16.5 (H-DFS).

The speedups of A-HTPGM compared to E-HTPGM and the baselines depend on the values of μ . On the tested datasets, the range and average speedups are: [1.1–21.3] and 5.2 (E-HTPGM), [3.4–203] and 25.1 (TPMiner), [6.4–1122] and 115.2 (IEMiner), and [9.3–1215] and 230.6 (H-DFS).

It is intuitive that A-HTPGM achieves high speedup when

μ is low (corresponds to few edges in the correlation graph), and low speedup when μ is high (more edges in the graph). However, the opposite trend holds for the accuracy (discussed in Section VI-C3): high accuracy if μ is high, and vice versa. Moreover, Table VII also shows that $\mu = 20\%$, 40% , and 60% yields similar speedup. Thus, we conclude that it is optimal to use high values of μ , e.g., 60% , since it yields both good performance and high accuracy.

Table VII also shows that A-HTPGM is most effective when the support and confidence thresholds σ and δ are low, e.g., $\sigma = 20\%$ and $\delta = 20\%$. This is because the number of pattern candidates with low support and confidence is large, and thus, it takes a long time to verify all candidates. Using A-HTPGM to prune uncorrelated time series, the majority of such pattern candidates are removed from the mining process.

TABLE IX: The Accuracy of A-HTPGM

| Support (%) | MI μ (%) | Confidence (%) | | | | | |
|-------------|--------------|----------------|-----|-----|------------|-----|-----|
| | | NIST | | | Smart City | | |
| | | 20 | 50 | 80 | 20 | 50 | 80 |
| 20 | 40% | 52 | 84 | 89 | 48 | 80 | 94 |
| | 60% | 72 | 85 | 89 | 69 | 81 | 94 |
| | 80% | 84 | 88 | 100 | 75 | 90 | 99 |
| | 90% | 99 | 100 | 100 | 100 | 100 | 100 |
| 50 | 40% | 80 | 90 | 100 | 76 | 85 | 96 |
| | 60% | 87 | 92 | 100 | 80 | 85 | 96 |
| | 80% | 91 | 94 | 100 | 92 | 96 | 100 |
| | 90% | 100 | 100 | 100 | 100 | 100 | 100 |
| 80 | 40% | 100 | 100 | 100 | 95 | 95 | 96 |
| | 60% | 100 | 100 | 100 | 96 | 96 | 96 |
| | 80% | 100 | 100 | 100 | 100 | 100 | 100 |
| | 90% | 100 | 100 | 100 | 100 | 100 | 100 |

On average, E-HTPGM consumes 3 times less memory than the baselines due to the applied pruning techniques, while A-HTPGM uses 5 times less memory than E-HTPGM and the baselines due to the pruning of uncorrelated time series.

2) *Evaluation of pruning techniques in E-HTPGM:* We evaluate the runtimes of E-HTPGM to understand how effective the proposed pruning techniques are. We compare different versions of E-HTPGM: (1) E-HTPGM with no pruning, (NoPrune)-E-HTPGM, (2) E-HTPGM with Apriori-based pruning (Lemmas 2, 3), (Apriori)-E-HTPGM, (3) E-HTPGM with transitivity-based pruning (Lemmas 4, 5, 6, 7), (Trans)-E-HTPGM, and (4) E-HTPGM with both pruning techniques applied, (All)-E-HTPGM.

The experiments are run on 3 different configurations: varying the data sizes, varying the confidence, and varying the support. The results are shown in Figs. 6 and 7 (the y-axis is in log scale). It can be seen that (All)-E-HTPGM achieves the best performance among all versions. Its speedup w.r.t. (NoPrune)-E-HTPGM ranges from 5 up to 60 depending on the configurations. This shows that the proposed pruning techniques are very effective in improving the performance of E-HTPGM. Furthermore, (Trans)-E-HTPGM is often more efficient than (Apriori)-E-HTPGM. The average speedup is from 3 to 12 for (Apriori)-E-HTPGM, and from 8 to 20 for (Trans)-E-HTPGM. However, applying both pruning always yields better speedup than applying either of them.

3) *Evaluation of A-HTPGM:* In this section, we analyze A-HTPGM from three aspects: (1) the accuracy of A-HTPGM, (2) the quality of patterns pruned by A-HTPGM, and (3) the trade-off between accuracy and runtime gain in A-HTPGM.

First, we compare the patterns extracted by A-HTPGM and E-HTPGM to evaluate the accuracy of A-HTPGM. Table IX shows the results. It can be seen that, A-HTPGM obtains low accuracy when μ is low ($\leq 40\%$), relatively high accuracy when $\mu = 60\%$, and high accuracy (more than 80% in most cases) when $\mu = 80\%$. A-HTPGM achieves 100% accuracy (most cases) when $\mu \geq 90\%$.

Next, we evaluate the quality of patterns which are pruned by A-HTPGM. These patterns are extracted from the uncorrelated time series. Fig. 8 shows the cumulative distribution of the confidences for the pruned patterns, using $\mu = 20\%$. It is seen that most of these patterns have low confidences: 80% have confidences less than 20% when the support is 10% and

20%, and 70% of patterns have confidences less than 30% when the support is 30%. These patterns are likely not very interesting to explore, and thus can be pruned.

Finally, we perform a trade-off analysis between the accuracy and the runtime gain as a means for choosing a proper value of μ . In Fig. 9, the accuracy and the runtime gain of A-HTPGM on the tested datasets are plotted together, with μ on the x-axis. We can see that, when $\mu < 60\%$, A-HTPGM obtains significant runtime gains ($\geq 80\%$), but significantly low accuracy ($\sim 25\%-75\%$). When $\mu \geq 60\%$, the accuracy is more than 80%, while the runtime gains are between 37%-90%. Based on this analysis, we conclude that low values of μ ($< 60\%$) are not optimal to use. Instead, μ should be high ($\geq 60\%$) to achieve both good performance and high accuracy.

4) *Scalability evaluation:* We proceed to evaluate the scalability of E-HTPGM and A-HTPGM on big datasets. First, based on the attributes of NIST, we generate more sequences to create a synthetic dataset that is 4 times bigger. Similarly for the Smart City dataset. We perform the experiments using two configurations: varying the data sizes (Figs. 10 and 11), and varying the number of attributes (Figs. 12 and 13).

Figs. 10, 11 show the runtimes of A-HTPGM, E-HTPGM and the baselines when the data size changes (y-axis in log scale). We can see, as the data size increases, the speedup between A-HTPGM and the baselines also increases. A-HTPGM achieves highest speedup with the largest data size (100% sequences) and lowest support and confidence (corresponding to largest search space). The range of the speedup growth rate of A-HTPGM w.r.t. the baselines is [0.3-1.24] on the tested datasets. The same trend is also applied to E-HTPGM, with the speedup growth rate is between [0.2-0.75].

Figs. 12 and 13 show the runtimes when changing the number of attributes (y-axis in log scale). It can be seen that, the speedups of A-HTPGM and E-HTPGM increase with the size of the attributes. A-HTPGM achieves the highest speedup with the largest number of attributes, and lowest support and confidence. The range of speedup growth rate is [0.12-2.93]. The same trend is also applied for E-HTPGM, with the speedup growth rate is between [0.11-0.77]. The scalability test shows that A-HTPGM and E-HTPGM can scale well on big datasets, both vertically (when the data size increases) and horizontally (when the number of attributes increases).

VII. CONCLUSION AND FUTURE WORK

In this paper, we present a comprehensive Frequent Temporal Pattern Mining from Time Series (FTPMfTS) solution that offers: (1) an end-to-end FTPMfTS process to mine frequent temporal patterns from time series, (2) an efficient and exact Hierarchical Temporal Pattern Graph Mining (E-HTPGM) algorithm that employs efficient data structures and different pruning techniques to achieve fast mining, and (3) an approximate A-HTPGM that uses mutual information to prune unpromising time series, allows HTPGM to scale on big datasets. Extensive experiments conducted on real-world datasets show that both A-HTPGM and E-HTPGM outperform the baselines, consume less memory, and scale well to big datasets. The approximate A-HTPGM achieves up to 3 orders

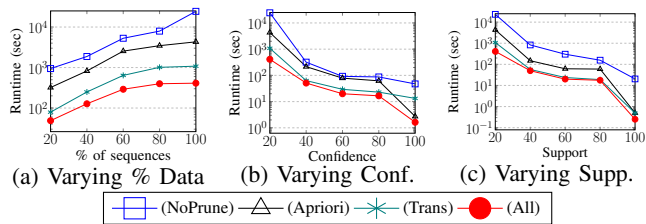


Fig. 6: Runtimes of E-HTPGM on NIST

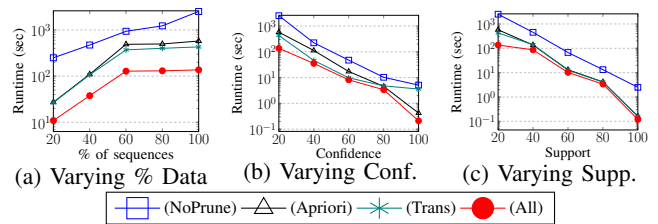


Fig. 7: Runtimes of E-HTPGM on Smart City

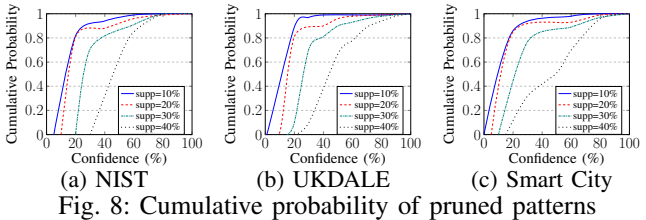


Fig. 8: Cumulative probability of pruned patterns

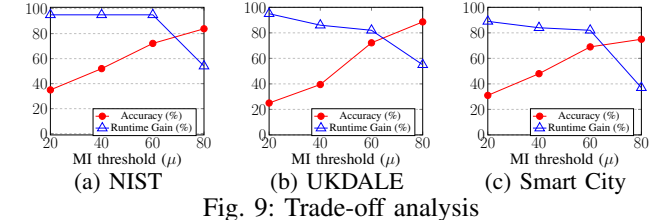


Fig. 9: Trade-off analysis

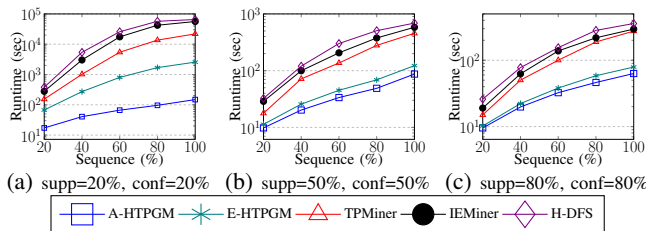


Fig. 10: Varying % of data on NIST

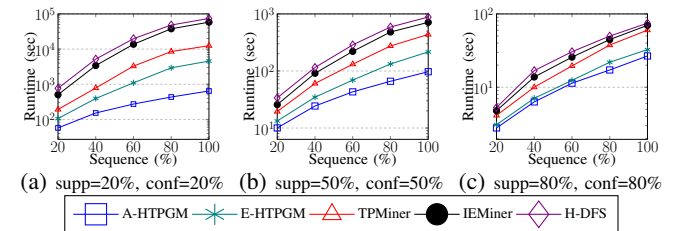


Fig. 11: Varying % of data on Smart City

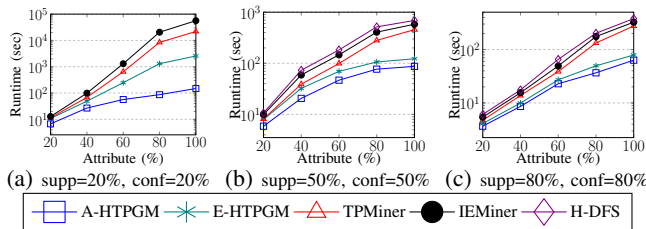


Fig. 12: Varying # of attributes on NIST

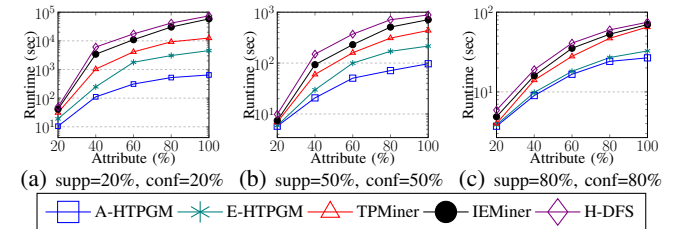


Fig. 13: Varying # of attributes on Smart City

of magnitude speedup compared to the baselines. In future work, we plan to extend HTPGM to perform pruning at the event level to further improve the performance.

REFERENCES

- [1] Y. Chen, W. Peng, and S. Lee, "Mining temporal patterns in time interval-based data," *TKDE*, vol. 27, 2015.
- [2] D. Patel, W. Hsu, and M. L. Lee, "Mining relationships among interval-based events for classification," in *SIGMOD*, 2008.
- [3] P. Papapetrou, G. Kollios, S. Sclaroff, and D. Gunopulos, "Mining frequent arrangements of temporal intervals," *KAIS*, vol. 21, 2009.
- [4] P.-s. Kam and A. W.-C. Fu, "Discovering temporal patterns for interval-based events," in *DaWak*, 2000.
- [5] S.-Y. Wu and Y.-L. Chen, "Mining nonambiguous temporal patterns for interval-based events," *TKDE*, vol. 19, 2007.
- [6] R. Moskovitch and Y. Shahar, "Fast time intervals mining using the transitivity of temporal relations," *KAIS*, vol. 42, 2015.
- [7] I. Batal, D. Fradkin, J. Harrison, F. Moerchen, and M. Hauskrecht, "Mining recent temporal patterns for event detection in multivariate time series data," in *SIGKDD*, 2012.
- [8] I. Batal, H. Valizadegan, G. F. Cooper, and M. Hauskrecht, "A temporal pattern mining approach for classifying electronic health record data," *TIST*, vol. 4, 2013.
- [9] E. A. Campbell, E. J. Bass, and A. J. Masino, "Temporal condition pattern mining in large, sparse electronic health record data: A case study in characterizing pediatric asthma," *JAMIA*, vol. 27, 2020.
- [10] A. U. Ahmed, C. F. Ahmed, M. Samiullah, N. Adnan, and C. K.-S. Leung, "Mining interesting patterns from uncertain databases," *Information Sciences*, vol. 354, 2016.

- [11] Y.-K. Lee, W.-Y. Kim, Y. D. Cai, and J. Han, "Comine: Efficient mining of correlated patterns," in *ICDM*, 2003.
- [12] Y. Ke, J. Cheng, and W. Ng, "Correlated pattern mining in quantitative databases," *TODS*, vol. 33, 2008.
- [13] J. Blanchard, F. Guillet, R. Gras, and H. Briand, "Using information-theoretic measures to assess association rule interestingness," in *ICDM'05*, 2005.
- [14] X. Cunjin, S. Wanjiiao, Q. Lijuan, D. Qing, and W. Xiaoyang, "A mutual-information-based mining method for marine abnormal association rules," *Computers & Geosciences*, vol. 76, 2015.
- [15] Y. Yao, "Information-theoretic measures for knowledge discovery and data mining," in *Entropy measures, maximum entropy principle and emerging applications*, 2003, pp. 115–136.
- [16] J. F. Allen, "Maintaining knowledge about temporal intervals," *Communications of the ACM*, vol. 26, 1983.
- [17] V. L. Ho, N. Ho, and T. B. Pedersen, "Efficient temporal pattern mining in big time series using mutual information," *arXiv preprint arXiv:2010.03653*, 2020. [Online]. Available: <https://arxiv.org/abs/2010.03653>
- [18] T. M. Cover and J. A. Thomas, *Elements of information theory*. John Wiley & Sons, 2012.
- [19] W. Healy, F. Omar, L. Ng, T. Ullah, W. Payne, B. Dougherty, and A. H. Fanney, (2018) Net zero energy residential test facility instrumented data. [Online]. Available: <https://pages.nist.gov/netzero/index.html/>
- [20] J. Kelly and W. Knottenbelt, "The UK-DALE dataset, domestic appliance-level electricity demand and whole-house demand from five UK homes," *Scientific Data*, 2015.
- [21] P. S. Data. (2016) Pecan street dataport. [Online]. Available: <https://www.pecanstreet.org/dataport/>

[22] N. Y. City. (2019) Nyc opendata. [Online]. Available: <https://opendata.cityofnewyork.us/>

APPENDIX

DETAILED PROOFS OF COMPLEXITIES, LEMMAS AND THEOREMS

A. Proof of the complexity of frequent single event mining

Complexity: The complexity of finding frequent events is $O(m \cdot |\mathcal{D}_{SEQ}|)$, where m is the number of distinct events.

Proof. Computing the support for each event E_i takes $O(|\mathcal{D}_{SEQ}|)$ (to count the set bits of the *bitmap* b_{E_i} of length $|\mathcal{D}_{SEQ}|$). Thus, counting the support for m events takes $O(m \cdot |\mathcal{D}_{SEQ}|)$. \square

B. Proof of Lemma 1

Lemma 1. *Let m be the number of distinct events in \mathcal{D}_{SEQ} , and h be the longest length of a temporal pattern. The total number of temporal patterns in HPG from L_1 to L_h is $O(m^h 3^{h^2})$.*

Proof. At L_1 , the number of nodes is: $N_1 = m \sim O(m)$. At L_2 , the number of permutations of m distinct events taken 2 at a time is: $P(m, 2)$. However, since the same event can form a pair of events with itself, e.g., (KOn, KOn), the total number of nodes at L_2 is: $N_2 = P(m, 2) + m \sim O(m^2)$. Each node in N_2 can form 3 different temporal relations, and thus, the total number of 2-event patterns in L_2 is: $N_2 \times 3^1 \sim O(m^2 3^1)$. Similarly, the number of 3-event nodes at L_3 is: $N_3 = P(m, 3) + P(m, 2) + m \sim O(m^3)$, and the number of 3-event patterns is: $N_3 \times 3^3 \sim O(m^3 3^3)$. At level L_h , the number of nodes is $O(m^h)$, while the number of h -event patterns is $O(m^h \times 3^{\frac{1}{2}h(h-1)}) \sim O(m^h 3^{h^2})$. Therefore, the total number of temporal patterns from L_1 to L_h in HPG is $O(m) + O(m^2 3^1) + O(m^3 3^3) + \dots + O(m^h 3^{h^2}) \sim O(m^h 3^{h^2})$. \square

C. Proof of Lemma 2

Lemma 2. *Let (E_i, E_j) be a pair of events occurs in a 2-event pattern P . Then, $\text{supp}(P) \leq \text{supp}(E_i, E_j)$.*

Proof. Derived directly from Defs. 3.11, 3.12, 3.13 and 3.14. \square

D. Proof of Lemma 3

Lemma 3. *Let (E_i, E_j) be a pair of events occurs in a 2-event pattern P . Then $\text{conf}(P) \leq \text{conf}(E_i, E_j)$.*

Proof. Can derived directly from Defs. 3.15 and 3.16. \square

E. Proof of the complexity of frequent 2-event pattern mining

Complexity: Let m be the number of frequent single events in L_1 , and i be the average number of event instances of each frequent event. The complexity of frequent 2-event pattern mining is $O(m^2 i^2 |\mathcal{D}_{SEQ}|^2)$.

Proof. The Cartesian product of m events in L_1 generates m^2 event pairs. To compute the support of m^2 event pairs, we count the set bits of the *bitmap* that takes $O(m^2 |\mathcal{D}_{SEQ}|)$.

For each node in L_2 , we need to compute the support and confidence of their temporal relations, which takes $O(i^2 |\mathcal{D}_{SEQ}|^2)$. We have potentially m^2 nodes. And thus, it takes $O(m^2 i^2 |\mathcal{D}_{SEQ}|^2)$.

The overall complexity is: $O(m^2 |\mathcal{D}_{SEQ}| + m^2 i^2 |\mathcal{D}_{SEQ}|^2) \sim O(m^2 i^2 |\mathcal{D}_{SEQ}|^2)$. \square

F. Proof of Lemma 4.

Lemma 4 *Let $S = \langle e_1, \dots, e_{n-1} \rangle$ be a temporal sequence that supports an $(n-1)$ -event pattern $P = \langle (E_{1 \triangleright e_1}, r_{12}, E_{2 \triangleright e_2}), \dots, (E_{n-2 \triangleright e_{n-2}}, r_{(n-2)(n-1)}, E_{n-1 \triangleright e_{n-1}}) \rangle$.*

Let e_n be a new event instance that is added to S to create a temporal sequence $S' = \langle e_1, \dots, e_n \rangle$. Then the set of temporal relations \mathfrak{R} is transitive on S' : $\forall e_i \in S', i \neq n, \exists r \in \mathfrak{R}$ s.t. $r(E_{i \triangleright e_i}, E_{n \triangleright e_n})$ holds.

Proof. Since $S' = \langle e_1, \dots, e_n \rangle$ is a temporal sequence, the event instances in S' are chronologically ordered by their start times. Then, $\forall e_i \in S', i \neq n: t_{s_i} \leq t_{s_n}$. We have:

- If $t_{e_i} \pm \epsilon \leq t_{s_n}$, then $E_{i \triangleright e_i} \rightarrow E_{n \triangleright e_n}$.
- If $(t_{s_i} \leq t_{s_n}) \wedge (t_{e_i} \pm \epsilon \geq t_{e_n})$, then $E_{i \triangleright e_i} \not\triangleright E_{n \triangleright e_n}$.
- If $(t_{s_i} < t_{s_n}) \wedge (t_{e_i} \pm \epsilon < t_{e_n}) \wedge (t_{e_i} - t_{s_n} \geq d_o \pm \epsilon)$ where d_o is the minimal overlapping duration, then $E_{i \triangleright e_i} \not\bowtie E_{n \triangleright e_n}$. \square

G. Proof of Lemma 5

Lemma 5. *Let $N_{k-1} = (E_1, \dots, E_{k-1})$ be a frequent combination of $(k-1)$ events, and E_k be a frequent single event. The combination $N_k = N_{k-1} \cup E_k$ cannot form any frequent k -event temporal patterns if $\nexists E_i \in N_{k-1}, r \in \mathfrak{R}$ s.t. $r(E_i, E_k)$ is a frequent temporal relation.*

Proof. Let p_k be any k -event pattern formed by N_k . Then p_k is a list of $\frac{1}{2}k(k-1)$ triples (E_i, r_{ij}, E_j) where each represents a relation $r(E_i, E_j)$ between two events. In order for p_k to be frequent, each of the relations in p_k must be frequent (Defs. 3.11 and 3.15, and Lemma 4). However, since $\nexists E_i \in N_{k-1}$ such that $r(E_i, E_k)$ is frequent, p_k is not frequent. \square

H. Proof of Lemma 6

Lemma 6. *Let P and P' be two temporal patterns. If $P' \subseteq P$, then $\text{conf}(P') \geq \text{conf}(P)$.*

Proof. Can be derived directly from Def. 3.16. \square

I. Proof of Lemma 7

Lemma 7. *Let P and P' be two temporal patterns. If $P' \subseteq P$ and $\frac{\text{supp}(P')}{\max_{1 \leq k \leq |P|} \{\text{supp}(E_k)\}} \leq \delta$, then $\text{conf}(P) \leq \delta$.*

Proof. We have:

$$\begin{aligned} \text{conf}(P) &= \frac{\text{supp}(P)}{\max_{1 \leq k \leq |P|} \{\text{supp}(E_k)\}} \\ &\leq \frac{\text{supp}(P')}{\max_{1 \leq k \leq |P|} \{\text{supp}(E_k)\}} \leq \delta \end{aligned}$$

\square

J. Proof of the complexity of frequent k-event pattern mining

Complexity: Let r be the average number of frequent (k-1)-event patterns in L_{k-1} . The complexity of frequent k-event pattern mining is $O(|IFreq| \cdot |L_{k-1}| \cdot r \cdot k^2 \cdot |\mathcal{D}_{SEQ}|)$.

Proof. For each frequent (k-1)-event pattern of a node in L_k , we need to compute the support and confidence of $\frac{1}{2}(k-1)(k-2)$ triples, which takes $O(\frac{1}{2}(k-1)(k-2)|\mathcal{D}_{SEQ}|) \sim O(k^2|\mathcal{D}_{SEQ}|)$.

We have $|IFreq| \times |L_{k-1}|$ nodes in L_k , each has r frequent (k-1)-event patterns. Thus, the total complexity is: $O(|IFreq| \cdot |L_{k-1}| \cdot r \cdot k^2 \cdot |\mathcal{D}_{SEQ}|)$. \square

K. Proof of Lemma 8

Lemma 8. Let $\text{supp}(X_1, Y_1)_{\mathcal{D}_{SYB}}$ and $\text{supp}(X_1, Y_1)_{\mathcal{D}_{SEQ}}$ be the supports of (X_1, Y_1) in \mathcal{D}_{SYB} and \mathcal{D}_{SEQ} , respectively. We have: $\text{supp}(X_1, Y_1)_{\mathcal{D}_{SYB}} \leq \text{supp}(X_1, Y_1)_{\mathcal{D}_{SEQ}}$.

Proof. Recall that when converting \mathcal{D}_{SYB} to \mathcal{D}_{SEQ} , we divide the symbolic time series in \mathcal{D}_{SYB} into equal length temporal sequences. Let n be the length of each symbolic time series in \mathcal{D}_{SYB} , and m be the length of each temporal sequence. The number of temporal sequences obtained in \mathcal{D}_{SEQ} is: $\lceil \frac{n}{m} \rceil$.

The support of (X_1, Y_1) in \mathcal{D}_{SYB} is computed as:

$$\text{supp}(X_1, Y_1)_{\mathcal{D}_{SYB}} = \frac{\sum_{i=1}^{\lceil \frac{n}{m} \rceil} \sum_{j=1}^m s_{ij}}{n} \quad (12)$$

where

$$s_{ij} = \begin{cases} 1, & \text{if } (X_1, Y_1) \text{ occurs in row } j \text{ of the sequence } s_i \text{ in } \mathcal{D}_{SYB} \\ 0, & \text{otherwise} \end{cases}$$

Intuitively, Eq. 12 computes the relative support of (X_1, Y_1) in \mathcal{D}_{SYB} by counting the number of times (X_1, Y_1) occurs in \mathcal{D}_{SYB} , and then dividing to the size of \mathcal{D}_{SYB} .

On the other hand, the support of (X_1, Y_1) in \mathcal{D}_{SEQ} is computed by counting the number of sequences in \mathcal{D}_{SEQ} that (X_1, Y_1) occurs. Note that if (X_1, Y_1) occurs more than one in the same sequence, we will count only 1 for that sequence. Thus, we have:

$$\text{supp}(X_1, Y_1)_{\mathcal{D}_{SEQ}} = \frac{\sum_{i=1}^{\lceil \frac{n}{m} \rceil} g_i}{n/m} = \frac{m \cdot \sum_{i=1}^{\lceil \frac{n}{m} \rceil} g_i}{n} \quad (13)$$

where

$$g_i = \begin{cases} 1, & \text{if } (X_1, Y_1) \text{ occurs in the sequence } g_i \text{ in } \mathcal{D}_{SEQ} \\ 0, & \text{otherwise} \end{cases}$$

Compare Eqs. 12 and 13, we have:

$$\sum_{i=1}^{\lceil \frac{n}{m} \rceil} \sum_{j=1}^m s_{ij} \leq m \cdot \sum_{i=1}^{\lceil \frac{n}{m} \rceil} g_i \quad (14)$$

Hence:

$$\text{supp}(X_1, Y_1)_{\mathcal{D}_{SYB}} \leq \text{supp}(X_1, Y_1)_{\mathcal{D}_{SEQ}} \quad (15)$$

\square

L. Proof of Theorem 1

Theorem 1. (Confidence lower bound) Let σ and μ be the support and the mutual information thresholds, respectively. Assume that (X_1, Y_1) is frequent in \mathcal{D}_{SYB} , i.e., $\text{supp}(X_1, Y_1)_{\mathcal{D}_{SYB}} \geq \sigma$. If $\tilde{I}(\mathcal{X}_S; \mathcal{Y}_S) \geq \mu$, then $\text{conf}(X_1, Y_1)_{\mathcal{D}_{SEQ}} \geq LB$ where

$$LB = \left(\sigma^{\sigma_m} \cdot \left(\frac{1 - \sigma_m}{n_x - 1} \right)^{1 - \sigma} \right)^{\frac{1 - \mu}{\sigma}} \cdot \frac{\sigma}{2 \cdot \sigma_m - \sigma} \quad (16)$$

where n_x is the number of symbols in the symbol alphabet Σ_X , and σ_m be the maximum support of (X_1, Y_1) in \mathcal{D}_{SYB} .

Proof. From Eq. (10), we have:

$$\tilde{I}(\mathcal{X}_S; \mathcal{Y}_S) = 1 - \frac{H(\mathcal{X}_S | \mathcal{Y}_S)}{H(\mathcal{X}_S)} \geq \mu \quad (17)$$

Hence:

$$\frac{H(\mathcal{X}_S | \mathcal{Y}_S)}{H(\mathcal{X}_S)} \leq 1 - \mu \quad (18)$$

First, we derive a lower bound for $\frac{H(\mathcal{X}_S | \mathcal{Y}_S)}{H(\mathcal{X}_S)}$.

$$\begin{aligned} \frac{H(\mathcal{X}_S | \mathcal{Y}_S)}{H(\mathcal{X}_S)} &= \frac{p(X_1, Y_1) \cdot \log p(X_1 | Y_1)}{p(X_1) \cdot \log p(X_1) + \sum_{i \neq 1} p(X_i) \cdot \log p(X_i)} \\ &+ \frac{\sum_{i \neq 1 \& j \neq 1} p(X_i, Y_j) \cdot \log \frac{p(X_i, Y_j)}{p(Y_j)}}{p(X_1) \cdot \log p(X_1) + \sum_{i \neq 1} p(X_i) \cdot \log p(X_i)} \end{aligned} \quad (19)$$

Applying the log sum inequality [18] for the second term of the denominator in Eq. (19), we get:

$$\begin{aligned} \sum_{i \neq 1} p(X_i) \cdot \log p(X_i) &\geq \sum_{i \neq 1} p(X_i) \log \frac{\sum_{i \neq 1} p(X_i)}{\sum_{i \neq 1} 1} \quad (20) \\ &= (1 - p(X_1)) \cdot \log \frac{1 - p(X_1)}{n_x - 1} \quad (21) \end{aligned}$$

Replace Eq. (21) into Eq. (19), we get:

$$\frac{H(\mathcal{X}_S | \mathcal{Y}_S)}{H(\mathcal{X}_S)} \geq \frac{p(X_1, Y_1) \cdot \log p(X_1 | Y_1)}{p(X_1) \cdot \log p(X_1) + (1 - p(X_1)) \cdot \log \frac{1 - p(X_1)}{n_x - 1}} \quad (22)$$

* **Case 1:** Assuming that $\text{supp}(Y_1)_{\mathcal{D}_{SYB}} \geq \text{supp}(X_1)_{\mathcal{D}_{SYB}}$. Thus, the confidence of (X_1, Y_1) in \mathcal{D}_{SYB} is computed as

$$\text{conf}(X_1, Y_1)_{\mathcal{D}_{SYB}} = \frac{\text{supp}(X_1, Y_1)_{\mathcal{D}_{SYB}}}{\text{supp}(Y_1)_{\mathcal{D}_{SYB}}} = \frac{p(X_1, Y_1)}{p(Y_1)} \quad (23)$$

Since we have: $\log \frac{p(X_1, Y_1)}{p(Y_1)} < 0$, and $\sigma \leq p(X_1, Y_1)$, we can deduce:

$$p(X_1, Y_1) \cdot \log \frac{p(X_1, Y_1)}{p(Y_1)} \leq \sigma \cdot \log \frac{p(X_1, Y_1)}{p(Y_1)} \quad (24)$$

We also have: $\log \sigma \leq \log p(X_1) < 0$, and $p(X_1) \leq \sigma_m$, hence:

$$p(X_1) \cdot \log p(X_1) \geq \sigma_m \cdot \log \sigma \quad (25)$$

We also get: $\log \frac{1-\sigma_m}{n_x-1} \leq \log \frac{1-p(X_1)}{n_x-1} < 0$, and $(1-p(X_1)) \leq (1-\sigma)$, hence:

$$(1-p(X_1)) \cdot \log \frac{1-p(X_1)}{n_x-1} \geq (1-\sigma) \cdot \log \frac{1-\sigma_m}{n_x-1} \quad (26)$$

From Eqs. (25), (26), we have:

$$\begin{aligned} p(X_1) \cdot \log p(X_1) + (1-p(X_1)) \cdot \log \frac{1-p(X_1)}{n_x-1} &\geq \\ \sigma_m \cdot \log \sigma + (1-\sigma) \cdot \log \frac{1-\sigma_m}{n_x-1} &\quad (27) \end{aligned}$$

Replace Eq. (24) into the numerator, and Eq. (27) into the denominator of Eq. (22), we get:

$$\frac{H(\mathcal{X}_S|\mathcal{Y}_S)}{H(\mathcal{X}_S)} \geq \frac{\sigma \cdot \log \frac{p(X_1, Y_1)}{p(Y_1)}}{\sigma_m \cdot \log \sigma + (1-\sigma) \cdot \log \frac{1-\sigma_m}{n_x-1}} \quad (28)$$

From Eqs. (18) and (28), it follows that:

$$(1-\mu) \geq \frac{\sigma \cdot \log \frac{p(X_1, Y_1)}{p(Y_1)}}{\sigma_m \cdot \log \sigma + (1-\sigma) \cdot \log \frac{1-\sigma_m}{n_x-1}} \quad (29)$$

$$\Rightarrow \text{conf}(X_1, Y_1)_{\mathcal{D}_{\text{SYB}}} = \frac{p(X_1, Y_1)}{p(Y_1)} \quad (30)$$

$$\geq \left(\sigma^{\sigma_m} \cdot \left(\frac{1-\sigma_m}{n_x-1} \right)^{1-\sigma} \right)^{\frac{1-\mu}{\sigma}} \quad (31)$$

* **Case 2:** Assuming that $\text{supp}(Y_1)_{\mathcal{D}_{\text{SYB}}} < \text{supp}(X_1)_{\mathcal{D}_{\text{SYB}}}$. Thus, the confidence of (X_1, Y_1) in \mathcal{D}_{SYB} is computed as

$$\text{conf}(X_1, Y_1)_{\mathcal{D}_{\text{SYB}}} = \frac{p(X_1, Y_1)}{p(X_1)} \quad (32)$$

From Eq. (22), we have:

$$\frac{H(\mathcal{X}_S|\mathcal{Y}_S)}{H(\mathcal{X}_S)} \geq \frac{p(X_1, Y_1) \cdot \log \left(\frac{p(X_1, Y_1)}{p(X_1)} \cdot \frac{p(X_1)}{p(Y_1)} \right)}{p(X_1) \cdot \log p(X_1) + (1-p(X_1)) \cdot \log \frac{1-p(X_1)}{n_x-1}} \quad (33)$$

$$\geq \frac{\sigma \cdot \log \left(\frac{p(X_1, Y_1)}{p(X_1)} \cdot \frac{\sigma_m}{\sigma} \right)}{\sigma_m \cdot \log \sigma + (1-\sigma) \cdot \log \frac{1-\sigma_m}{n_x-1}} \quad (34)$$

From Eqs. (18), (34), it follows that:

$$(1-\mu) \geq \frac{\sigma \cdot \log \left(\frac{p(X_1, Y_1)}{p(X_1)} \cdot \frac{\sigma_m}{\sigma} \right)}{\sigma_m \cdot \log \sigma + (1-\sigma) \cdot \log \frac{1-\sigma_m}{n_x-1}} \quad (35)$$

$$\Rightarrow \text{conf}(X_1, Y_1)_{\mathcal{D}_{\text{SYB}}} = \frac{p(X_1, Y_1)}{p(X_1)} \quad (36)$$

$$\geq \left(\sigma^{\sigma_m} \cdot \left(\frac{1-\sigma_m}{n_x-1} \right)^{1-\sigma} \right)^{\frac{1-\mu}{\sigma}} \cdot \left(\frac{\sigma}{\sigma_m} \right) \quad (37)$$

In Eq. (37), we have $\frac{\sigma}{\sigma_m} < 1$. Thus, from Eqs. (31), (37), we

have the confidence lower bound of (X_1, Y_1) in \mathcal{D}_{SYB} in both cases is:

$$\text{conf}(X_1, Y_1)_{\mathcal{D}_{\text{SYB}}} \geq \left(\sigma^{\sigma_m} \cdot \left(\frac{1-\sigma_m}{n_x-1} \right)^{1-\sigma} \right)^{\frac{1-\mu}{\sigma}} \quad (38)$$

Next, we consider the confidence of (X_1, Y_1) in the temporal sequence database \mathcal{D}_{SEQ} . From Lemma 8, we have:

$$\text{supp}(X_1)_{\mathcal{D}_{\text{SYB}}} \leq \text{supp}(X_1)_{\mathcal{D}_{\text{SEQ}}} \leq \sigma_m \quad (39)$$

$$\Rightarrow \text{supp}(X_1)_{\mathcal{D}_{\text{SYB}}} + \beta_1 \leq \sigma_m \quad (40)$$

$$\Rightarrow \beta_1 \leq \sigma_m - \sigma \quad (41)$$

where β_1 is a non-negative number, and $\text{supp}(X_1)_{\mathcal{D}_{\text{SYB}}} \geq \sigma$. Without loss of generality, we assume that $\text{supp}(X_1)_{\mathcal{D}_{\text{SEQ}}} \geq \text{supp}(Y_1)_{\mathcal{D}_{\text{SEQ}}}$. Thus, the confidence of (X_1, Y_1) in \mathcal{D}_{SEQ} is computed as

$$\text{conf}(X_1, Y_1)_{\mathcal{D}_{\text{SEQ}}} = \frac{\text{supp}(X_1, Y_1)_{\mathcal{D}_{\text{SEQ}}}}{\text{supp}(X_1)_{\mathcal{D}_{\text{SEQ}}}} \geq \frac{\text{supp}(X_1, Y_1)_{\mathcal{D}_{\text{SYB}}}}{\text{supp}(X_1)_{\mathcal{D}_{\text{SYB}}} + \beta_2} \quad (42)$$

From Eqs. (41), (42), we have:

$$\text{conf}(X_1, Y_1)_{\mathcal{D}_{\text{SEQ}}} \geq \frac{\text{supp}(X_1, Y_1)_{\mathcal{D}_{\text{SYB}}}}{\text{supp}(X_1)_{\mathcal{D}_{\text{SYB}}} + \sigma_m - \sigma} \quad (43)$$

From Eq. 38, we get:

$$\begin{aligned} \text{conf}(X_1, Y_1)_{\mathcal{D}_{\text{SYB}}} &= \frac{\text{supp}(X_1, Y_1)_{\mathcal{D}_{\text{SYB}}}}{\text{supp}(X_1)_{\mathcal{D}_{\text{SYB}}}} \\ &\geq \left(\sigma^{\sigma_m} \cdot \left(\frac{1-\sigma_m}{n_x-1} \right)^{1-\sigma} \right)^{\frac{1-\mu}{\sigma}} \quad (44) \end{aligned}$$

Let:

$$l = \left(\sigma^{\sigma_m} \cdot \left(\frac{1-\sigma_m}{n_x-1} \right)^{1-\sigma} \right)^{\frac{1-\mu}{\sigma}} \quad (45)$$

From Eqs. (43), (44), (45), we have:

$$\begin{aligned} \frac{\text{supp}(X_1, Y_1)_{\mathcal{D}_{\text{SYB}}}}{\text{supp}(X_1)_{\mathcal{D}_{\text{SYB}}} + \sigma_m - \sigma} &\geq \frac{l \cdot \text{supp}(X_1)_{\mathcal{D}_{\text{SYB}}}}{\text{supp}(X_1)_{\mathcal{D}_{\text{SYB}}} + \sigma_m - \sigma} \quad (46) \\ &\geq \frac{l \cdot \sigma}{\sigma_m + \sigma_m - \sigma} = \frac{l \cdot \sigma}{2 \cdot \sigma_m - \sigma} \quad (47) \end{aligned}$$

Finally, from Eqs. (43) and (47), we can conclude:

$$\text{conf}(X_1, Y_1)_{\mathcal{D}_{\text{SEQ}}} \geq \left(\sigma^{\sigma_m} \cdot \left(\frac{1-\sigma_m}{n_x-1} \right)^{1-\sigma} \right)^{\frac{1-\mu}{\sigma}} \cdot \frac{\sigma}{2 \cdot \sigma_m - \sigma} \quad \square$$